6992–7008 *Nucleic Acids Research, 2013, Vol. 41, No. 14* *Published online 30 May 2013*
doi:10.1093/nar/gkt447

Prospero-related homeobox 1 (Prox1) functions as a novel modulator of retinoic acid-related orphan receptors α- and γ-mediated transactivation

Yukimasa Takeda and Anton M. Jetten*

Division of Intramural Research, Cell Biology Section, National Institute of Environmental Health Sciences, National Institutes of Health, 111 T.W. Alexander Drive, Research Triangle Park, NC 27709, USA

Received February 13, 2013; Revised April 30, 2013; Accepted May 2, 2013

ABSTRACT

In this study, we identify Prospero-related homeobox 1 (Prox1) as a novel co-repressor of the retinoic acid-related orphan receptors, RORα and RORγ. Prox1 interacts directly with RORγ and RORα and negatively regulates their transcriptional activity. The AF2 domain of RORs is essential for the interaction, whereas Prox1 interacts with RORs through either its 28 amino acids N-terminal region or its C-terminal prospero-like domain. RORγ antagonists stabilize the interaction between RORγ and Prox1. The homeodomain and the interaction through the prospero-like domain of Prox1 are critical for its repression of ROR transcriptional activity. Chromatin immunoprecipitation analysis demonstrated that in liver, Prox1 is recruited to the ROR response element sites of the clock genes, brain and muscle Arnt-like protein 1 (*Bmal1*), neuronal PAS domain protein 2 (*Npas2*) and cryptochrome 1 (*Cry1*), as part of the same complex as RORs. Knockdown of Prox1 by siRNAs in human hepatoma Huh-7 cells increased the expression of RORγ and several ROR-target genes, along with increased histone acetylation at these ROR response element sites. Chromatin immunoprecipitation sequencing analysis suggests that Prox1 is a potential ROR target gene in liver, which is supported by the regulation of the rhythmic expression of Prox1 by RORγ. Our data suggest that Prox1 is part of a feedback loop that negatively regulates the transcriptional control of clock and metabolic networks by RORs.

INTRODUCTION

The retinoic acid-related orphan receptors, RORα–γ (NR1F1-3), members of the nuclear receptor superfamily, function as ligand-dependent transcription factors that are involved in the regulation of a wide range of physiological processes and have been associated with several pathologies (1–5). In addition to regulatory functions in cerebellar and lymph node development, thymopoiesis and Th17 differentiation, RORα and RORγ have been implicated in the regulation of circadian rhythm and various metabolic pathways. RORs play a role in the regulation of the circadian expression of several clock genes, including brain and muscle Arnt-like protein 1 (*Bmal1*), neuronal PAS domain protein 2 (*Npas2*), cryptochrome 1 (*Cry1*) and circadian locomotor output cycles kaput (*Clock*), and various metabolic genes (6–14). RORα/γ also regulates the hepatic expression of Phase I and Phase II enzymes (15,16) and exhibits a critical role in the regulation of glucose and lipid metabolism in several tissues (17–20). Mice deficient in RORα exhibit a greatly reduced susceptibility to diet- and age-induced obesity, liver steatosis and insulin resistance, whereas reduced RORγ expression in humans and mice is associated with increased insulin sensitivity (21,22). Recently, single-nucleotide polymorphisms in RORs have been linked to increased risk of several pathologies in humans, including type two diabetes, asthma, bipolar disorder and celiac disease (23–26).

RORs regulate transcription by binding as monomers to ROR response elements (ROREs), consisting of AGGT CA preceded by an AT-rich sequence, in the regulatory region of target genes. Transcriptional regulation by RORs is mediated through interaction with co-repressors and co-activators, including NCOR1, RIP140, NCOA1 and PGC-1α (4,27–29). A yeast two-hybrid analysis using the ligand-binding domain (LBD) of RORα as bait identified Prospero-related homeobox one (Prox1) as a potential interacting partner of RORα (27). However, this potential interaction has not been further characterized. Prox1 contains at its C-terminus an atypical homeodomain and an adjacent prospero-like domain (30–34). In *Drosophila*, the prospero domain regulates the nuclear localization of *Prospero* by masking a

*To whom correspondence should be addressed. Tel: +1 919 541 2768; Fax: +1 919 541 4133; Email: jetten@niehs.nih.gov

nuclear export signal within the homeodomain. Prox1 functions either as an activator of gene transcription by binding directly to specific DNA elements through its homeodomain or as a co-repressor (30,34,35). It can interact with several transcription factors, including HNF4α (36), SF1 (37) and Ets-1 (38). Prox1 plays a critical role in embryonic development and functions as a key regulatory protein in neurogenesis and the development of the heart, eye lens, liver, pancreas and the lymphatic system (39–43). Alterations in the expression or function of Prox1 have been implicated in several human cancers (30,44). Moreover, single-nucleotide polymorphisms in the *Prox1* gene have been linked to obesity and type two diabetes, suggesting an important role for Prox1 in the regulation of metabolic/endocrine functions (45–47).

In this study, we demonstrate by several approaches that both RORα and RORγ interact with Prox1. The AF2 domain of RORα or RORγ is essential for this interaction, whereas both the C- and N-terminus of Prox1 can interact with RORs. We further show that Prox1 represses ROR-mediated transcriptional activity and that the homeo/prospero-like domain is critical for this repression. Chromatin immunoprecipitation (ChIP) analysis indicated that this repression involves recruitment of Prox1 to the ROREs in the regulatory regions of ROR target genes in liver, including several clock and metabolic genes. In addition, we provide evidence that RORγ regulates the circadian pattern of expression of *Prox1* in liver, whereas chromatin immunoprecipitation sequencing (ChIP-Seq) analysis indicated that Prox1 is a direct RORγ target gene. Thus, our study identifies Prox1 as a novel repressor of ROR-mediated transcriptional regulation and suggests that Prox1 is part of a feedback loop that negatively modulates ROR transcriptional activity and, as such, the regulation of clock and metabolic networks by RORs.

MATERIALS AND METHODS

Experimental animals

Heterozygous C57/BL6 staggerer ($RORα^{+/sg}$) mice, a natural mutant strain containing a 6.5-kb deletion in *RORα* that exhibits a similar phenotype as mice with a targeted disruption of *RORα* (4,48), were purchased from Jackson Laboratories (Bar Harbor, ME, USA). C57/BL6 $RORγ^{-/-}$ mice were described previously (9,49). Mice were supplied *ad libitum* with NIH-A31 formula and water and maintained at 25°C on a constant 12-h light:12-h dark cycle. Littermate wild-type (WT) mice were used as control animals. All animal protocols followed the guidelines outlined by the NIH Guide for the Care and Use of Laboratory Animals and were approved by the Institutional Animal Care and Use Committee at the NIEHS.

Plasmids

Mouse *Prox1* cDNA was purchased from OriGene (Rockville, MD, USA). The pCMV10-3×Flag-RORγ, pCMV10-3xFlag-RORα, the corresponding ΔAF2 mutants, pM-RORγ, VP16-RORγ(LBD) and VP16-RORα(LBD) expression vectors were described previously (10,28). Prox1 and Prox1 mutants were generated by polymerase chain reaction (PCR) amplification and cDNA fragments inserted into the EcoRI and XhoI sites of pCMV-Myc and pEGFP-C1 (Clontech, Palo Alto, CA, USA), or the EcoRI and SalI sites of pMAL-c2X (New England BioLabs, Inc., Ipswich, MA, USA). Point mutations were generated by site-directed mutagenesis using the Quickchange Site Directed Mutagenesis Kit (Stratagene) following the manufacturer's protocol. To generate pLVX-mCherry-RORα/γ, the full-length region of RORα/γ was amplified by PCR and inserted into the XhoI and EcoRI sites of pLVX-mCherry-N1 (Clontech). All constructs were verified by restriction enzyme analysis and DNA sequencing.

Co-immunoprecipitation and western blot analysis

HEK293 cells were transiently transfected with pCMV10-3xFlag-RORα or -RORγ or their respective AF2-deletion mutants RORαΔAF2 and RORγΔAF2 and pCMV-Myc-Prox1 using Lipofectamine 2000 reagent (Invitrogen, Carlsbad, CA, USA). Cells were harvested 36–48 h after transfection in Tris-NaCl-EDTA (TNE) buffer (10 mM Tris–HCl, pH 7.8, 0.15 M NaCl, 1 mM ethylenediaminetetraacetic acid and 1% Nonidet P-40) containing phosphatase and protease inhibitor cocktails (Sigma-Aldrich, St. Louis, MO, USA). To evaluate the effects of RORγ antagonists on RORγ–Prox1 interaction, transfected cells were treated during the last 24 h with or without T0901317 or ursolic acid (Sigma-Aldrich) as indicated. Cell lysates were pre-absorbed with protein G beads or mouse IgG-agarose and subsequently incubated with an anti-Myc antibody (Invitrogen) for 2 h at 4°C and then for 1 h with protein G beads or with anti-Flag M2 affinity gel (Sigma-Aldrich). The beads were then washed five times with TNE buffer, and the immunoprecipitated proteins were examined by western blot analysis. To evaluate the stability of RORγ protein, HEK293 cells were transiently transfected with pCMV10-3xFlag-RORγ, pCMV-Myc-Prox1 or the indicated pCMV-Myc-Prox1 mutant using Lipofectamine 2000 (Invitrogen). Cells were treated with 10 μg/ml cycloheximide for 6 h before they were harvested. Proteins were subsequently examined by western blot analysis with anti-Flag M2 (Sigma-Aldrich), anti-Myc (Invitrogen) or anti-Gapdh antibody (Cell Signaling Technology, Danvers, MA, USA). All experiments were performed at least twice.

Maltose-binding protein pull-down assay

[^{35}S]methionine-labeled RORγ, RORγΔAF2 and RORγΔLBD proteins were generated using a TNT quick-coupled transcription/translation system (Promega, Madison, WI, USA). Different fragments of Prox1 were generated by PCR and inserted into the pMAL-c2X expression vector (New England BioLabs Inc.). Each maltose-binding protein (MBP)–Prox1 protein was expressed in bacteria, BL21(DE3)pLys (Agilent Biotechnologies, Santa Clara, CA, USA), purified with amylose resin (New England BioLabs Inc., Ipswich, MA, USA) and evaluated by sodium dodecyl sulfate–polyacrylamide gel electrophoresis (PAGE)

(Supplementary Figure S2). Equal amounts of amylose resin-bound MBP–Prox1 or MBP protein were incubated with radiolabeled RORγ in 0.2 ml binding buffer (20 mM Tris–HCl, pH 7.6, 100 mM KCl, 0.05% Nonidet P-40 (NP-40), 0.1 mM ethylenediaminetetraacetic acid, 10% glycerol, 0.2% Tween 20 and 1 mM phenylmethylsulfonyl fluoride). After 1-h incubation at 4°C, the beads were washed five times in binding buffer. Bound proteins were separated by PAGE and then visualized by autoradiography.

Confocal microscopy

COS-1 cells were plated in 35-mm glass-bottom dishes and 24 h later transfected with pEGFP-Prox1 and pCMV10-3xFlag-RORα or -RORγ, or with pLVX-RORγ-mCherry-N1 or -RORα-mCherry-N1 and the indicated pCMV-Myc-Prox1 mutants. Cells were fixed 24 h after transfection, and the subcellular localization was examined by immunofluorescent staining with anti-Flag M2 antibody and Alexa Fluor 594-conjugated goat anti-mouse IgG (Invitrogen) or an anti-Myc antibody and Alexa Fluor 488-conjugated goat anti-mouse IgG (Invitrogen). Fluorescence was observed with a Zeiss LSM 510 UV Meta confocal microscope. The percentage of cells in which Prox1 was predominantly localized to the nucleus (N) or cytoplasm (C) or equally distributed between the nucleus and cytoplasm (N + C) was calculated. When cells were co-transfected with Prox1 and RORγ, only cells expressing both proteins were counted. In every case, >100 cells were analyzed.

Reporter gene assay

Human hepatoma Huh-7 cells were co-transfected as indicated with pCMVβ-Gal, pCMV10-3xFlag-RORα or -RORγ, pCMV-Myc-Prox1 or a pCMV-Myc-Prox1 mutant and a pGL4.27-$(RORE)_5$ reporter plasmid containing 5× RORE, pGL4.10-*Npas2*(−1534/+81) containing the −1534/+81 region of the *Npas2* promoter, pGL4.10-*Bmal1*(−650/+105) or pGL4.27-*Cry1*(+22976/+23214) containing the respective RORE-regulatory region, using Lipofectamine 2000 (Invitrogen). For mammalian two-hybrid analysis, CHO-K1 cells were co-transfected with a pGL4.27-$(UAS)_5$ reporter plasmid, pCMV-β-Gal, pM-EBIP96 peptide (28), VP16-RORα(LBD) or VP16-RORγ(LBD) and different amounts of pCMV-Myc-Prox1 expression vector as indicated. For mammalian mono-hybrid analysis, CHO-K1 cells were co-transfected with a pGL4.27-$(UAS)_5$ reporter plasmid, pCMV-β-Gal and pM-RORγLBD. Mammalian two-hybrid analysis was carried out as described previously (50), Huh-7 cells were co-transfected with a pGL4.27-$(UAS)_5$, pCMV-β-Gal, pM-TIP27, VP16-TAK1 and different amounts of pCMV-Myc-Prox1. After 24-h incubation, the luciferase and β-galactosidase activities were measured by Luciferase Assay Substrate (Promega) and Luminescent β-galactosidase Detection Kit II (Clontech). All transfections were performed in triplicate and repeated at least twice.

Chromatin immunoprecipitation and formaldehyde-assisted isolation of regulatory elements analysis

The ChIP assay was performed using a ChIP assay kit from Millipore (Billerica, MA, USA) according to the manufacturer's protocol with minor modifications as described previously (9,10). In short, livers isolated from four WT, $RORα^{sg/sg}$, $RORγ^{-/-}$ and $RORα^{sg/sg}RORγ^{-/-}$ (DKO) mice at Zeitgeber time 20 (ZT20) were homogenized with a polytron PT 3000 (Brinkmann Instruments) and cross-linked by 1% formaldehyde for 20 min at room temperature. After a wash in phosphate-buffered saline, an aliquot of the cross-linked chromatin was sonicated and incubated overnight with an antibody against Prox1 (51043-1-AP; Proteintech Group Inc., Chicago, IL, USA), RORα or RORγ as described previously (10). Mouse IgG antibody was used as negative control. After incubation with protein G agarose beads for 2 h, DNA–protein complexes were eluted. The cross-links were reversed by overnight incubation at 65°C in the presence of 25 mM NaCl, digested with RNase A and proteinase K, and then the ChIPed-DNA was purified. The amount of the ChIPed-DNA relative to each input DNA was determined by quantitative PCR (QPCR). All QPCR reactions were carried out in triplicate. Sequences of primers for ChIP–QPCR were listed in Supplementary Table S2. Serial ChIP experiments were performed using an anti-Prox1 antibody for the first ChIP as described earlier in the text and an anti-RORα or RORγ antibody (sc-6062 and sc-28559, respectively, Santa Cruz Biotechnology, Santa Cruz, CA, USA) for the second ChIP. The amount of ChIPed-DNA relative to each input DNA was determined by QPCR. The ROR–DKO liver and the amplification of *Gapdh* served as negative control samples. Formaldehyde-assisted isolation of regulatory elements (FAIRE) analysis was performed as previously reported (10).

Knockdown of Prox1

Huh-7 cells were transfected with ON-TARGETplus SMARTpool human PROX1 (L-016913-00-0005, Thermo Scientific, Lafayette, CO, USA) or a negative universal control siRNA (46-2002, Invitrogen) by DharmaFECT Transfection Reagent four (Thermo Scientific) according to the manufacturer's instructions. The knockdown of endogenous *Prox1* mRNA and protein was examined, respectively, by QPCR and western blot analysis using an antibody against Prox1 or anti-Gapdh (Cell Signaling Technology), which served as an internal control. Cells were collected 3 days after transfection with control or Prox1 siRNA and used for QPCR, ChIP and FAIRE analysis. ChIP analysis was carried out with antibodies against Prox1, mouse IgG or histone H3 lysine 9 acetylation (H3K9Ace) (07–352; Millipore). QPCR, ChIP and FAIRE analyses were performed in triplicate.

Quantitative reverse transcriptase–PCR

Huh-7 cells were transfected with either control or *Prox1* siRNA. Three days later, cells were lysed directly in

RNeasy lysis buffer (RTL) buffer, and RNA was extracted using a QIAshredder column followed by RNeasy Mini kit (Qiagen, Valencia, CA, USA) according to the manufacturer's instructions. Primary cultures of mouse hepatocytes collected from *RORγ*$^{-/-}$ mice were infected with pLVX-mCherry-Empty (Clontech) or -RORγ lentivirus and 24 h later RNA was isolated. The RNA was reverse transcribed using High-Capacity cDNA Archive Kit (Applied Biosystems). Gene expression analysis was performed by quantitative reverse transcriptase (QRT)–PCR analysis with SYBR Green I or the TaqMan system (Applied Biosystems, Foster City, CA, USA). The reactions were carried out in triplicate in a 7300 Real Time PCR system (Applied Biosystems) using 20 ng of cDNA and the following conditions: 2 min at 45°C and 10 min at 95°C, followed by 40 cycles of 15 s at 95°C and 60 s at 60°C. All the results were normalized to the amount of *Gapdh* mRNA. Liver tissues were collected from WT, *RORγ*$^{-/-}$ and *RORα*$^{sg/sg}$ mice every 4 h over a period of 24 h as described previously (10). After homogenization in RLT buffer, RNA was extracted using RNeasy Mini kit (Qiagen). QPCR was performed to quantify circadian expression of *Prox1* mRNA in the same way described earlier in the text. Products specificity was routinely confirmed by melting curve analysis. QRT–PCR primer sequences were listed in Supplementary Table S1.

RESULTS

The AF2 domain of RORγ and RORα is required for their interaction with Prox1

Yeast two-hybrid analysis using the LBD of RORα as bait identified Prox1 as a potential RORα-interacting protein; however, no further analysis was carried out (27). In this study, we characterized in detail the interaction between RORs and Prox1 in HEK293 cells co-transfected with Myc-Prox1 and Flag-RORγ or Flag-RORα expression plasmids. Co-immunoprecipitation analysis with an anti-Myc antibody showed that Flag-RORγ co-immunoprecipitated with Myc-Prox1 (Figure 1A). However, the Flag-RORγΔAF2 mutant lacking the AF2 activation domain did not significantly co-immunoprecipitate with Myc-prox1. Similarly, Flag-RORα, but not the Flag-RORαΔAF2 mutant, co-immunoprecipitated with Myc-Prox1 (Figure 1B). These results indicated that both RORα and RORγ are able to interact with Prox1, and that the AF2 domain of RORs is critical for this interaction. Immunoprecipitation analysis was carried out in the inverse manner, immunoprecipitation (IP) with anti-Flag followed by immunoblotting with anti-Myc antibody, supported the interaction between Prox1 and RORs (Supplementary Figure S1A).

We further observed that the level of ROR protein was consistently increased when co-expressed with Prox1, whereas Myc-Prox1 protein was decreased when co-expressed with RORs (Figure 1A and B). We, therefore, examined whether these effects were related to changes in protein stability. RORγ protein was stabilized by co-expression with Prox1 (Figure 1C), whereas the stability of Prox1 protein was not significantly affected by co-expression with RORγ (Figure 1D), suggesting different mechanisms for regulation of expression of two proteins.

Interaction with (ant)agonists is known to induce changes in the conformation of the LBD domain of nuclear receptors and subsequently promote or inhibit the interactions with distinct transcriptional mediators. To determine whether ROR antagonists had any influence on the interaction between RORγ and Prox1, HEK293 cells were treated with the RORγ antagonists, T0901317 or ursolic acid (51,52), and their effect on this interaction was analyzed. Co-immunoprecipitation analysis indicated a stronger association between RORγ and Prox1 in the presence of an antagonist (Figure 1E), suggesting that ROR antagonists promote or stabilize the interaction between Prox1 and RORs.

Prox1 physically interacts with RORγ through its N- and C-terminal region

To determine which regions of Prox1 were important for its interaction with RORγ, the binding of [^{35}S]-labeled RORγ to a MBP–Prox1 fusion protein and different MBP-conjugated Prox1 fragments [N(1-106), M(107-340), M(341-573) and C(574-737)] (Supplementary Figure S2) was examined by pull-down analysis using amylose resin. As shown in Figure 2A, the N-terminus, as well as the C-terminus containing the homeo/prospero-like domain, was able to interact with RORγ, whereas the two middle sections of Prox1 [M(107-340) and M(341-573)] did not. Consistent with our co-immunoprecipitation results, the ROR mutants, RORγΔAF2 and RORγΔLBD, which lack the activation and ligand-binding domains, respectively, were unable to interact with any of these Prox1 fragments (Figure 1A and B). These data indicated that both the N- and C-terminus of Prox1 are able to interact directly with the LBD of RORs.

Previous studies have demonstrated that many co-repressors and co-activators interact with the AF2 domain of nuclear receptors through their LXXLL motifs (53,54). To determine whether the two LXXLL motifs at the N-terminus of Prox1 are required for its interaction with RORγ, the effect of mutations (L70A/L73A and I93A/L96A) within those motifs on the interaction of the Prox1 N-terminus N(1–106) with RORγ was examined. As shown in Figure 2A, the mutations in the LXXLL motifs had little effect on the interaction of N(1–106) with RORγ. Moreover, the N-terminal fragments N(1–66) and N(1–28), in which the LXXLL motifs were deleted, were still able to interact with RORγ (Figure 2B). These results indicate that the LXXLL motifs are dispensable for the interaction of Prox1 with RORγ, and that its N-terminus up to ^{28}Gly is sufficient to mediate the interaction.

The C-terminus of Prox1 contains a homeodomain (amino acids 574–635) and an adjacent prospero-like domain (amino acids 636–737), which play roles in DNA recognition and the regulation of the nuclear localization of Prox1 (30,32,35). To further characterize the necessity of each domain in ROR interaction, the ability of the C(574–635) and C(636–737) C-terminal regions to

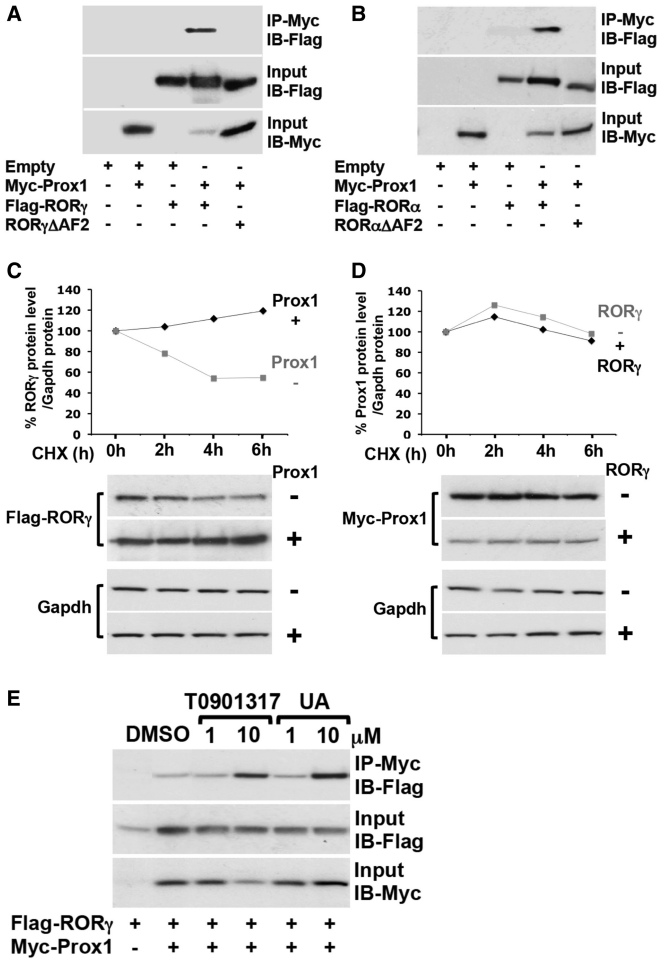

Figure 1. Prox1 interacts with the AF2 domain of RORα and RORγ. HEK293 cells were transfected with pCMV-Myc-Prox1 and pCMV10-3xFlag-RORγ(**A**) or -RORα (**B**) or the respective AF2 deletion mutant. Cell lysates were prepared and used for co-immunoprecipitation analysis with an anti-Myc antibody. Immunoprecipitated proteins were separated by PAGE and examined by western blot analysis with an anti-Flag antibody. (**C** and **D**) Prox1 enhances RORγ protein stability. HEK293 cells were transfected with pCMV-Myc-Prox1 and pCMV10-3xFlag-RORγ and 36 h later treated with 10 μg/ml cycloheximide for the times indicated. RORγ and Prox1 protein levels were normalized against the Gapdh loading and their level at 0 h (100%). Flag-RORγ (**C**) and Myc-Prox1 (**D**) were examined by western blot analysis, and the intensity of the bands was determined and plotted. (**E**) Prox1 interaction with RORγ was increased by RORγ antagonist treatment. HEK293 cells were co-transfected with pCMV-Myc-Prox1 and pCMV10-3xFlag-RORγ and then incubated with each ROR antagonists, T0901317 or ursolic acid, or dimethyl sulfoxide (DMSO) at 1 or 10 μM for the last 24 h. The amount of RORγ in complex with Prox1 was examined by co-immunoprecipitation/western blot analysis as described earlier in the text. The level of total Flag-RORγ and Myc-Prox1 (input) was also analyzed.

interact with RORγ was investigated. Figure 2B shows that RORγ was able to interact with the prospero-like domain C(636–737) but not with the homeodomain C(574–635). Moreover, two homeodomain mutations, N626A and R628A [C(574-737)m], which abolish the ability of Prox1 to bind DNA (55), did not affect the interaction with RORγ (Figure 2A). These results suggest that the interaction of Prox1 with RORγ involves the prospero-like domain and does not require the DNA-binding function of Prox1.

To investigate whether the N- and/or C-terminus of Prox1, regions that interact with RORγ were necessary for its stabilizing action on RORγ (Figure 1C), the effects of PΔN106, PΔC636 and PΔN106ΔC636 on RORγ stability were compared. Figure 2C shows that PΔN106 and PΔN106ΔC636 were expressed at considerably higher levels than full-length Prox1 and PΔC636. This difference was not related to changes in transfection efficiency. Thus, these data indicate that deletion of the N-terminus influenced the level of Prox1 protein expression and suggest that the N-terminus might regulate Prox1 protein level possibly through a (post)translational mechanism. Compared with full-length Prox1, PΔN106 increased the level of RORγ to a considerably smaller degree despite its higher level of expression, whereas PΔC636 and PΔN106ΔC636 had no significant effect on RORγ protein level. These data indicated that loss of its N-terminus and particularly its C-terminus diminished the stabilizing effect of Prox1 on RORγ.

RORs can promote the nuclear localization of Prox1

To examine the effect of RORs on the subcellular localization of Prox1, COS-1 cells were transfected with Flag-RORγ and/or EGFP–Prox1 expression plasmids, and the localization of the proteins was examined by immunofluorescent staining. When expressed alone, both RORγ and Prox1 were largely localized to the nucleus, and when expressed together, the two proteins co-localized to the same nuclear foci (Figure 3A). The 3D imaging confirmed the co-localization of Prox1 and RORγ in the nucleus (Supplementary Figure S1B). A similar co-localization was observed with Flag–RORα (Figure 3A and Supplementary Figure S1B); however, no significant overlap was observed between EGFP–Prox1 and Flag–TAK1, a nuclear receptor that does not interact with Prox1 (data not shown).

Next, we examined the effect of various N- and C-terminal deletions in Prox1 on its co-localization with RORγ (Figure 3B). When expressed alone, full-length Prox1 and the N-terminal deletion mutant PΔN106 localized principally to the nucleus in, respectively, 70 and 50% of the cells (Figure 3C and D), whereas co-expression with RORγ enhanced their nuclear localization to, respectively, 100 and 90% of the cells. Consistent with a previous study of *Drosophila Prospero* (32), which showed that the C-terminus plays a major role in regulating the nuclear localization of Prox1, the C-terminal deletion mutant PΔC636 was localized to the nucleus in only 6% of the cells; however, when co-expressed with RORγ, its nuclear localization was greatly increased and PΔC636 localized predominantly to the nucleus in 80% of the cells (Figure 3E). In contrast, the Prox1 mutant PΔN106ΔC636, lacking both the N- and C- terminus, was localized predominantly to the cytoplasm and co-expression with RORγ did not enhance its nuclear localization significantly (Figure 3F). Moreover, RORγ was able to promote the nuclear translocation of C-terminal Prox1 deletion mutant,

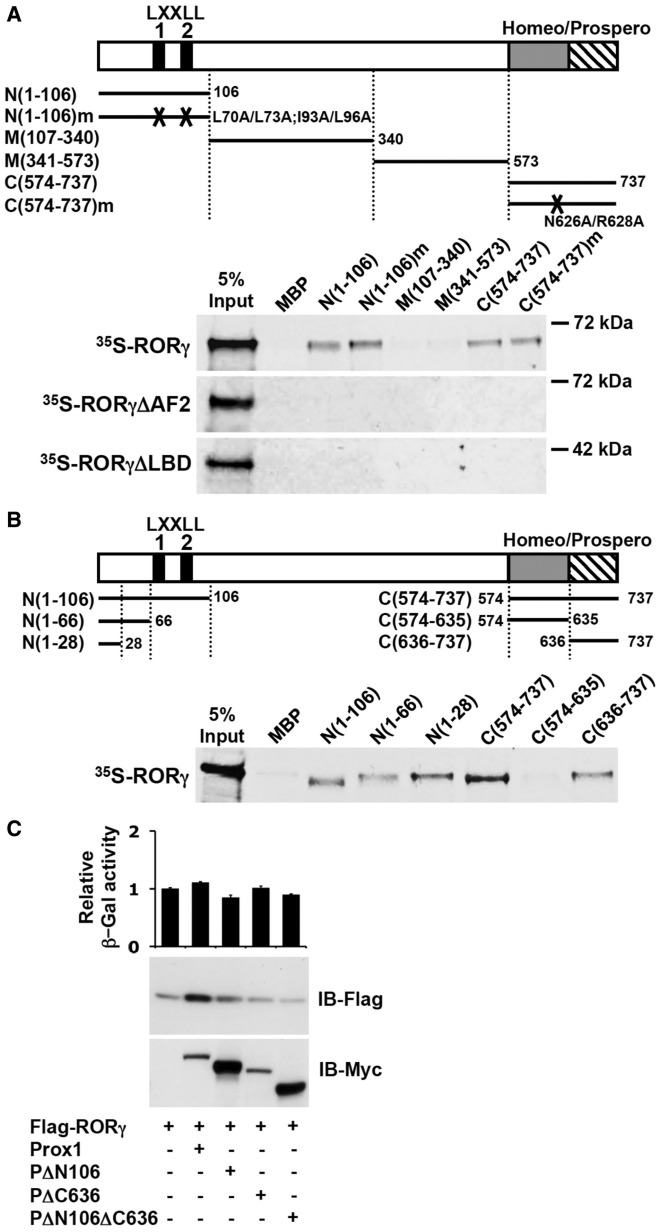

Figure 2. Both the N- and C-terminus of Prox1 are able to interact with RORγ. (**A**) MBP pull-down assays were performed using radiolabeled ^{35}S-RORγ (full-length), ^{35}S-RORγΔAF2 lacking the AF2 domain, ^{35}S-RORγΔLBD lacking the LBD and a series of MBP–Prox1 fragments, N(1-106), N(1-106)m, M(107-340), M(341-573), C(574-737) and C(574-737)m, as shown in the schematic. After incubation with amylose resin, MBP–Prox1 complexes were analyzed by PAGE, and radiolabeled RORγ was detected by autoradiography. Five percent of the input of each radiolabeled RORγ was loaded in the first lane. MBP was used as negative control. (**B**) MBP pull-down assays were performed using radiolabeled full-length RORγ (^{35}S-RORγ) and several N- and C-terminal fragments of Prox1, N(1-106), N(1-66), N(1-28), C(574-737), C(574-635) and C(636-737) as shown in the schematic. Samples were processed as described under A. (**C**) Loss of the N- and C-terminus of Prox1 diminishes its stabilizing effect on RORγ protein. HEK293 cells were transfected with pCMV10-3xFlag-RORγ and the pCMV-Myc-Prox1 or the pCMV-Myc-Prox1 mutant indicated and the level of RORγ and Myc-Prox1 protein examined by western blot analysis. Co-transfection with a β-Gal reporter indicated no significant difference in transfection efficiency between cells transfected with different Prox1 mutants.

P(LXXLL)mΔC636, in which the LXXLL motifs are mutated, but not that of PΔN28ΔC636 (Supplementary Figure S3A and B). These data are consistent with the conclusion that the LXXLL motifs of Prox1 are dispensable, and that either its N-terminal 28 amino acids or prospero-like domain can support the interaction with RORγ.

To narrow down the region in the Prox1 C-terminus required for RORγ interaction, we analyzed the mutants PΔN106ΔC716, PΔN106ΔC722 and PΔN106ΔC729 containing shorter C-terminal deletions (Figure 3B). PΔN106ΔC716 and PΔN106ΔC722 largely localized to the cytoplasm, whereas PΔN106ΔC729 was found predominantly in the nucleus (Figure 3G–I). Co-expression with RORγ had little effect on the cytoplasmic localization of PΔN106ΔC716 and PΔN106ΔC722, but promoted the nuclear localization of PΔN106ΔC729. These data are consistent with our conclusion that both the C- and N-terminus of Prox1 can mediate its interaction with RORγ, and that the interaction with RORγ promotes the accumulation of Prox1 in the nucleus. Moreover, this analysis indicated that the region between ^{723}Glu and ^{729}Asn at the C-terminus of Prox1 is required for its nuclear localization and interaction with RORγ.

Transcriptional activation by RORα and RORγ is repressed by Prox1

To investigate whether Prox1 influences ROR transcriptional activity, the effect of Prox1 on ROR-mediated activation of the Luc reporter gene under the control of either $(RORE)_5$ or the ROREs of the ROR target genes, *Npas2, Cry1* and *Bmal1* (9), was examined in human hepatoma Huh-7 cells. Prox1 inhibited the activation of $(RORE)_5$-Luc by RORα and RORγ in a dose-dependent manner (Figure 4A) and repressed ROR-induced activation of the *Npas2* promoter, *Npas2*(−1534/+81), to a similar extent (Figure 4B). Prox1 also inhibited the *Bmal1*(RORE)- and *Cry1*(RORE)-dependent transactivation by RORγ (Supplementary Figure S4A). Prox1 did not significantly repress the transcriptional activation by VP16-TAK1, suggesting that the repression by Prox1 is not because of a general effect on the basic transcriptional machinery, but it is selective (Supplementary Figure S4B). Inhibition of RORγ-mediated transactivation was supported by mono-hybrid analysis, which showed that Prox1 significantly inhibited the activation of the upstream activation sequence (UAS)-driven Luc reporter gene by Gal4(DBD)-RORγ(LBD) (Figure 4C). Transcriptional activation by RORs is mediated by co-activators that interact with the ROR(LBD) through their LXXLL motif(s) (28). Mammalian two-hybrid analysis, in which activation of the UAS-driven Luc reporter is dependent on the interaction between Gal4(DBD)-LXXLL(EBIP96) and VP16-RORα(LBD) or VP16-RORγ(LBD), demonstrated that co-expression with Prox1 greatly repressed this activation, suggesting that Prox1 inhibited this interaction (Figure 4D). Because the LXXLL motifs of Prox1 are not required for ROR interaction, this inhibition seems not to be because of direct competition between the Prox1 LXXLL motifs and LXXLL(EBIP96) for ROR(LBD)

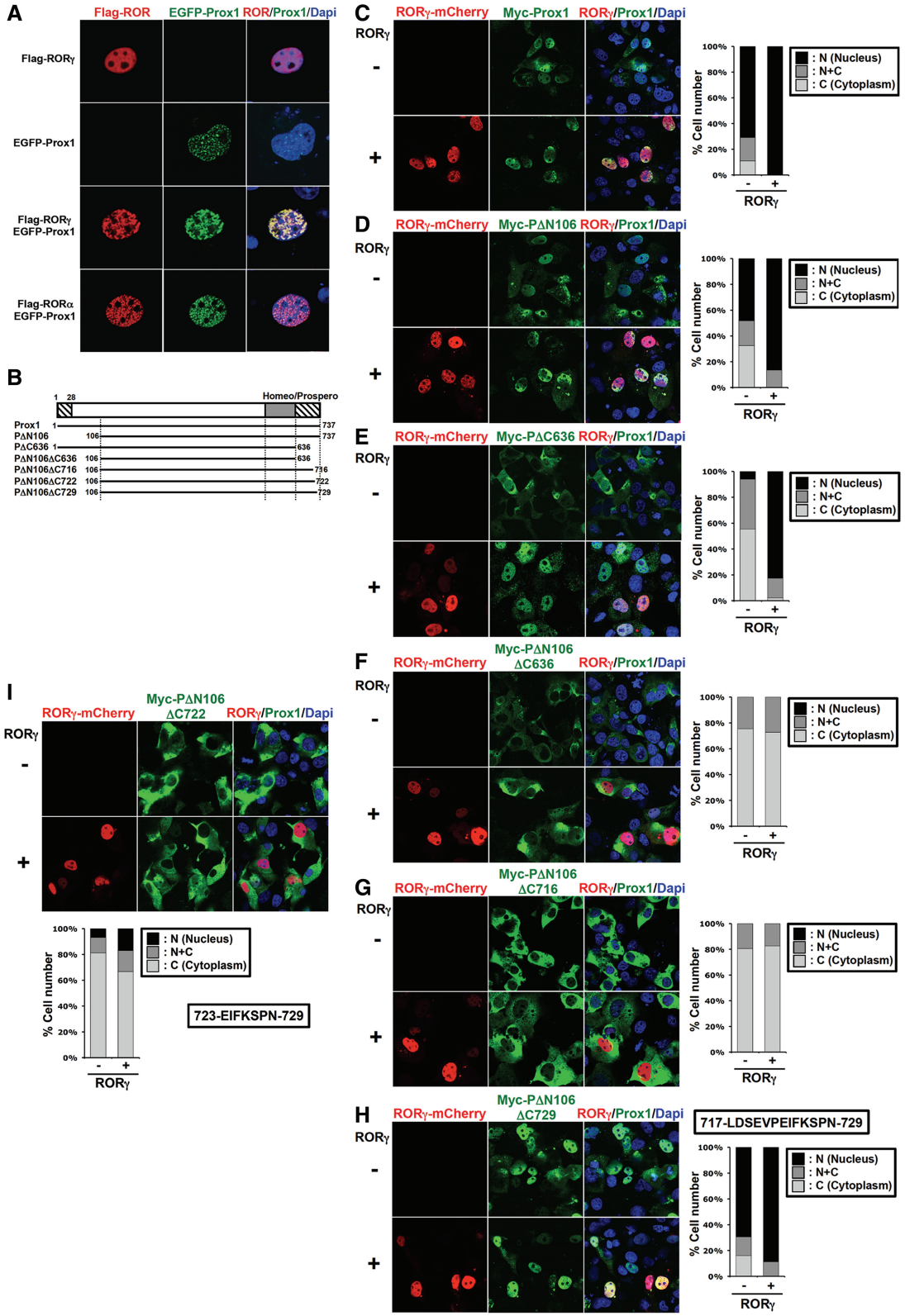

Figure 3. RORγ promotes translocation of Prox1 into the nucleus through the N- and C-terminus of Prox1. (**A**) Co-localization of Prox1 and RORγ or RORα. COS-1 cells were transfected with pEGFP-Prox1 and pCMV10-3xFlag-RORγ or -RORα as indicated. After immunohistochemical staining with anti-Flag M2 antibody and 4,6-diamidino-2-phenylindole (DAPI), immunofluorescence was examined by confocal microscopy. (**B**) Schematic presentation of a series of N- and C-terminal Prox1 deletion mutants. (**C–I**) COS-1 cells were transfected with pLVX-RORγ-mCherry-N1 and pCMV-Myc expression plasmids containing Prox1 or the N- or C-terminal mutants, PΔN106, PΔC636, PΔN106ΔC636, PΔN106ΔC716, PΔN106ΔC729 or PΔN106ΔC722. Subsequently, their subcellular localization was examined as described under A. The percentage of cells in which Prox1 was predominantly localized in the nucleus (N) or in the cytoplasm (C) or distributed equally between nucleus and cytoplasm (N + C) was calculated. In cells co-transfected with both RORγ and Prox1, only cells ($n > 100$) in which both RORγ and Prox1 were co-expressed were counted.

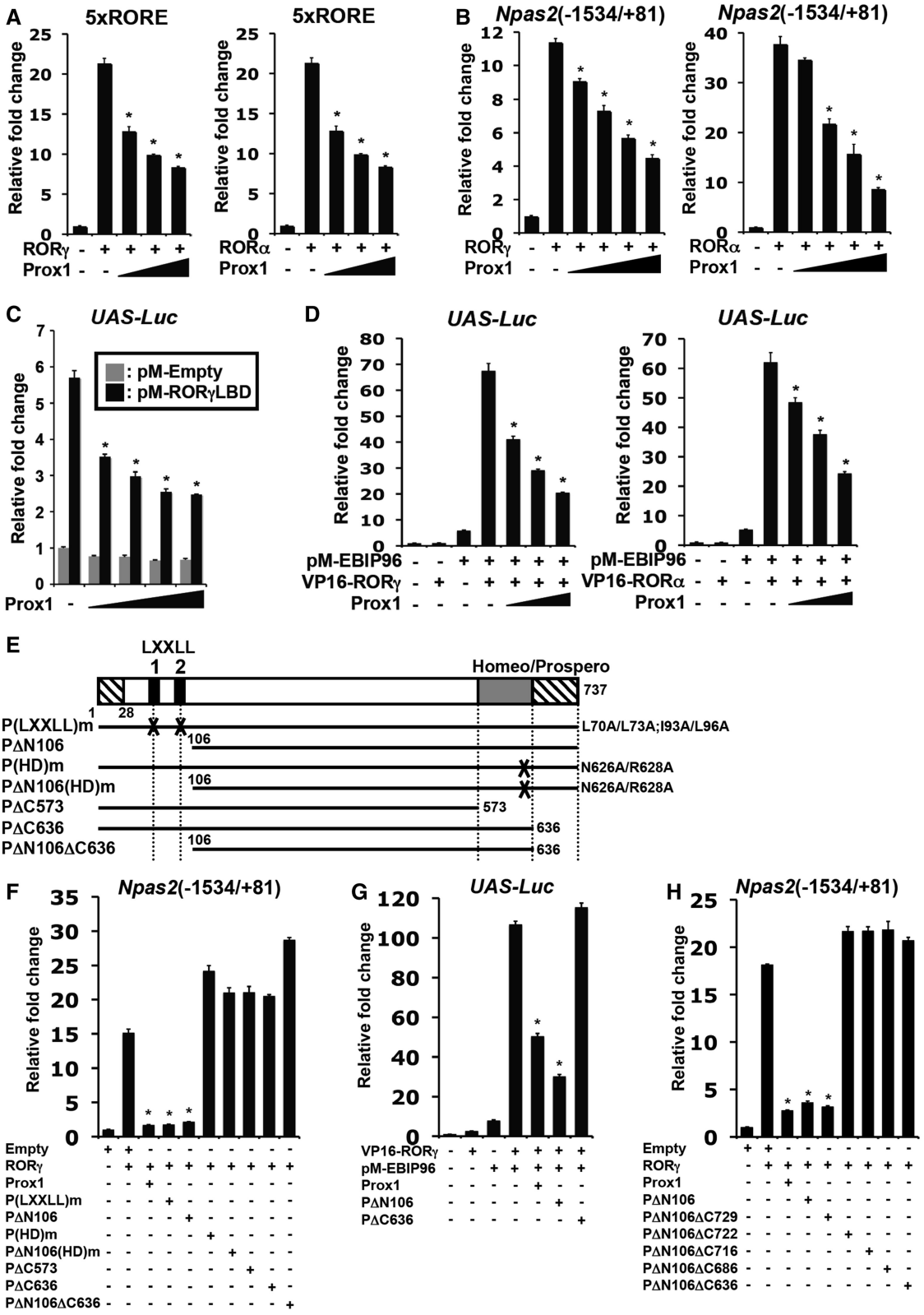

Figure 4. Prox1 represses RORγ- and RORα-mediated transcriptional activation. (**A**) Huh-7 cells were co-transfected with the pGL4.27-$(RORE)_5$ or pGL4.10-*Npas2*(-1534/+81) reporter plasmid, pCMV-β-Gal, pCMV10-3xFlag-RORγ or -RORα, and increasing amounts of pCMV-Myc-Prox1 expression plasmid (ROR:Prox1 = 1:0.2, 1:0.5, 1:1). Luciferase and β-galactosidase activities were measured 24 h later. (**B**) Huh-7 cells were co-transfected with pGL4.10 reporter plasmid containing *Npas2* promoter region (−1534/+81) and expression vectors as described earlier in the text. (**C**) Mammalian monohybrid analysis. CHO cells were transfected with pGL4.27-$(UAS)_5$ reporter plasmid containing UAS, pCMV-β-Gal, pM-RORγLBD and increasing amounts of pCMV-Myc-Prox1 expression plasmid (ROR:Prox1 ratios are 1:0.1, 1:0.2, 1:0.5 and 1:1). (**D**) Mammalian two-hybrid analysis. CHO cells were transfected with pGL4.27-$(UAS)_5$, pCMV-β-Gal, pM-GAL4-LXXLL(EBIP96),

(continued)

binding. Our data suggest that the binding of Prox1 to RORs disrupts the interaction of RORs with co-activators.

To determine what regions in Prox1 are required for the repression of RORγ-mediated transactivation, the effect of several Prox1 mutants on the activation of the *Npas2* promoter by RORγ was examined (Figure 4E and F). The N-terminal Prox1 mutants P(LXXLL)m and PΔN106, in which the LXXLL sites were either mutated or deleted, repressed the activation of the *Npas2* promoter by RORγ to a similar extent as WT Prox1. The C-terminal deletion mutants, PΔC573 and PΔC636, did not suppress *Npas2* promoter activation (Figure 4F) or the activation of a UAS-driven Luc reporter by Gal4(DBD)-LXXLL(EBIP96) and VP16-RORγ(LBD) (Figure 4G). These data suggest that a functional homeo/prospero-like domain is required for Prox1-mediated repression of RORγ transcriptional activity and are in agreement with the conclusion that the LXXLL motifs are dispensable. The requirement for a functional homeodomain was supported by data showing that the homeodomain mutants, P(HD)m and PΔN106(HD)m, did not repress RORγ-mediated transactivation (Figure 4F). RORγ was still able to promote the nuclear localization of PΔN106(HD)m (Supplementary Figure S3C), suggesting the failure of PΔN106(HD)m to repress RORγ activity was not because of its inability to interact with RORγ. To narrow down the region within the prospero-like domain required for this repression three additional deletions mutants, PΔN106ΔC686, PΔN106ΔC716, PΔN106ΔC722 and PΔN106ΔC729, were analyzed. Figure 4H shows that only the PΔN106ΔC729 mutant was able to repress RORγ-mediated transcriptional activation. These data are consistent with our conclusion that the region between ^{723}Glu and ^{729}Asn in the prospero-like domain is required for Prox1 interaction with RORγ and repression of its transcriptional activity. This region is also needed for the increased nuclear localization of Prox1 by RORγ (Figure 3G–I).

Prox1 is recruited to the RORE of clock genes *in vivo* in a circadian manner

Recently, we reported that the regulation of the circadian expression of several clock and metabolic genes by RORγ involves recruitment of RORγ to ROREs in their respective regulatory regions in phase with the peak expression of RORγ (9,10). To examine whether Prox1 is recruited to these ROREs, we performed ChIP analysis using an anti-Prox1 antibody and chromatin from livers collected at ZT22 from WT and RORγ-deficient mice. A non-specific IgG antibody and the *Gapdh* promoter were used as negative control samples. Figure 5A shows that Prox1 was recruited to the RORE sites in the regulatory regions of *Bmal1*, *Npas2* and *Cry1*. Prox1 was also associated with the *Pepck* promoter, which is not an RORγ target and was used as a positive control to analyze Prox1 recruitment (56). The association of Prox1 was significantly reduced in RORγ-deficient liver; however, recruitment to the *Pepck* and *Gapdh* promoters was not significantly different between WT and RORγ-deficient liver. These results suggest that the recruitment of Prox1 to the RORE-containing regulatory regions of *Bmal1*, *Npas2* and *Cry1*, but not the association with the *Pepck* promoter, was RORγ-dependent. The loss of RORγ did not totally abolish the association of Prox1 with the ROREs in *Bmal1*, *Npas2* and *Cry1*; this residual association might be related to Prox1 recruitment by RORα, which also binds these ROREs (9,10). Because RORγ exhibits an oscillatory pattern of expression with a peak expression at ZT18-22 and the lowest expression at ZT6-10, we compared Prox1 recruitment between these two ZTs. Figure 5B shows that the association of Prox1 at the RORE sites of *Bmal1*, *Npas2* and *Cry1* genes was higher at ZT20, when RORγ is most highly expressed (10), than at ZT8. No significant difference in the recruitment of Prox1 was observed to the *Gapdh* promoter between ZT8 and ZT20, which served as a negative control. These results suggest that association of Prox1 with the ROREs in these clock genes is partially mediated through recruitment by RORγ and dependent on the circadian time. This conclusion was further supported by Re-ChIP analysis using chromatin from livers of WT, *RORγ*- or *RORα*-deficient mice, an anti-Prox1 in the first and either anti-RORγ or RORα antibody in the second ChIP. The data suggest that both Prox1 and RORs are in the same complex at the ROREs of *Bmal1*, *Npas2* and *Cry1* (Figure 5C).

Prox1 modulates transcription of ROR-direct target genes

Because Prox1 represses RORγ-mediated transactivation, we hypothesized that downregulation of Prox1 might enhance the expression of RORγ target genes. As both RORγ and Prox1 are highly expressed in liver (57), we examined the effect of Prox1 knockdown on the expression of RORγ target genes in human hepatoma Huh-7 cells. Prox1 knockdown by respective siRNAs reduced *Prox1* mRNA expression and Prox1 protein levels by

Figure 4. Continued
VP16-RORγ(LBD) or -RORα(LBD) and increasing amounts of pCMV-Myc-Prox1 (ROR:Prox1 = 1:0.2, 1:0.5, 1:1). Luciferase and β-galactosidase activities were measured 24 h later. (**E**) Schematic presentation of several N- or C-terminal Prox1 deletion constructs and mutants containing mutations in the LXXLL motifs or the homeodomain. (**F**) Huh-7 cells were co-transfected with pGL4.10-*Npas2*(-1534/+81), pCMV-β-Gal, pCMV10-3xFlag-RORγ and pCMV-Myc expression vector containing Prox1 or the Prox1 mutants P(LXXLL)m, PΔN106, P(HD)m, PΔN106(HD)m, PΔC573, PΔC636 and PΔN106ΔC636) as indicated. (**G**) Mammalian two-hybrid analysis. CHO cells were transfected with pGL4.27-$(UAS)_5$, pCMV-β-Gal, pM-GAL4-LXXLL(EBIP96), VP16-RORγ(LBD) and pCMV-Myc expression vector containing Prox1, PΔN106 or PΔC636. (**H**) The region of Prox1 between amino acids 723 and 729 is required for its repression of RORγ-mediated transactivation of *Npas2*(−1534/+81). Huh-7 cells were transfected with pGL4.10-*Npas2*(-1534/+81), pCMV-β-Gal, pCMV10-3xFlag-RORγ and pCMV-Myc expression vector containing Prox1, PΔN106, PΔN106ΔC729, PΔN106ΔC722, PΔN106ΔC716, PΔN106ΔC686 or PΔN106ΔC636, as indicated. Luciferase and β-galactosidase activities were measured 24 h later. All the experiments were performed in triplicate. Data represent mean ± SEM; $^*P < 0.05$ by ANOVA.

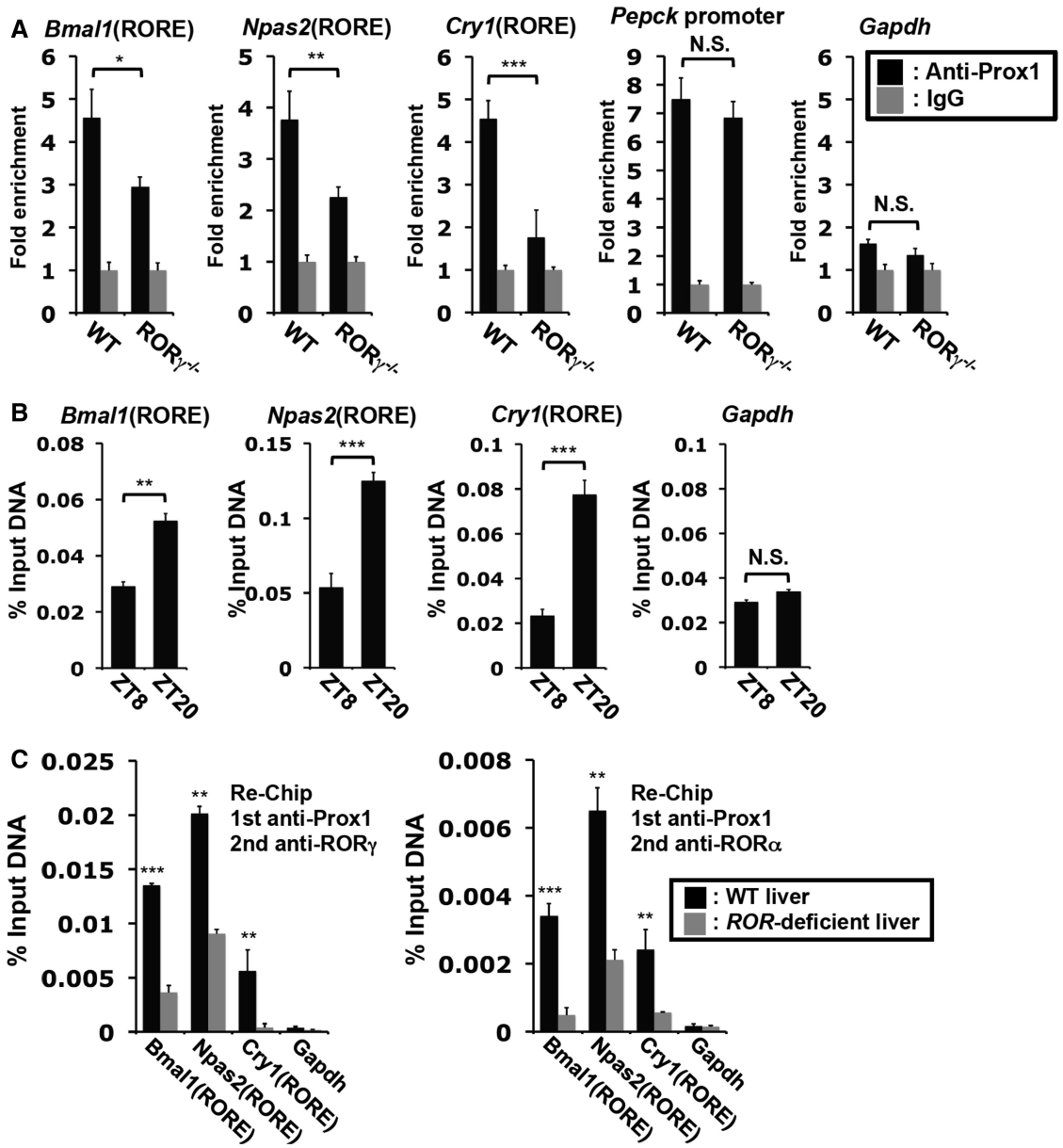

Figure 5. Prox1 is recruited to the RORE sites of ROR-target clock genes *in vivo*. (**A**) ChIP–QPCR was performed using an anti-Prox1 antibody and chromatin prepared from liver collected at ZT22 from WT and $ROR\gamma^{-/-}$ mice ($n = 4$). Fold enrichment as percentage of input DNA was calculated. The *Pepck* promoter, which is not a RORγ target, was used as a positive control for Prox1 recruitment. Amplification of *Gapdh* served as a negative control. (**B**) ChIP–QPCR was performed using anti-Prox1 antibody and chromatin prepared from the livers ($n = 4$) collected from WT mice at ZT8 and ZT20. The recruitment of Prox1 to the REREs of *Bmal1*, *Npas2* and *Cry1* was analyzed. (**C**) Re-ChIP analysis was performed with chromatin prepared from WT and *ROR*-deficient livers ($n = 4$) collected at ZT20. The chromatin was immunoprecipitated with anti-Prox1 antibody first, then the extract was further immunoprecipitated with either anti-RORα or anti-RORγ antibody. Data represent mean ± SEM; $^{*}P < 0.05$, $^{**}P < 0.01$, $^{***}P < 0.001$ by ANOVA.

~80% (Figure 6A) and significantly enhanced the expression of several RORγ target genes, including the clock genes *Bmal1*, *Npas2*, *Cry1* and the metabolic genes, arginine vasopressin receptor 1 a (*Avpr1a*) and elongation of very long chain fatty acid 3 (*Elovl3*) (Figure 6B). The expression of the Prox1-regulated gene *Pepck* (56), which served as a positive control, was also enhanced. The increased expression of the three clock genes was accompanied by reduced association of Prox1 with the respective RORE regulatory regions (Figure 6C). In addition, downregulation of Prox1 expression enhanced the activation of the Luc reporter under the control of the RORE-containing regulatory region of the *Bmal1*(−650/+105), *Npas2*(−1534/+81) or *Cry1*(+22976/+23214) (Figure 6D). Interestingly, Prox1 knockdown also increased the expression of *RORγ* mRNA, suggesting that in addition to its effect on RORγ transcriptional activity, Prox1 might function as a potential repressor of *RORγ* transcription (Figure 6B). Thus, the increased expression of RORγ target genes observed after Prox1

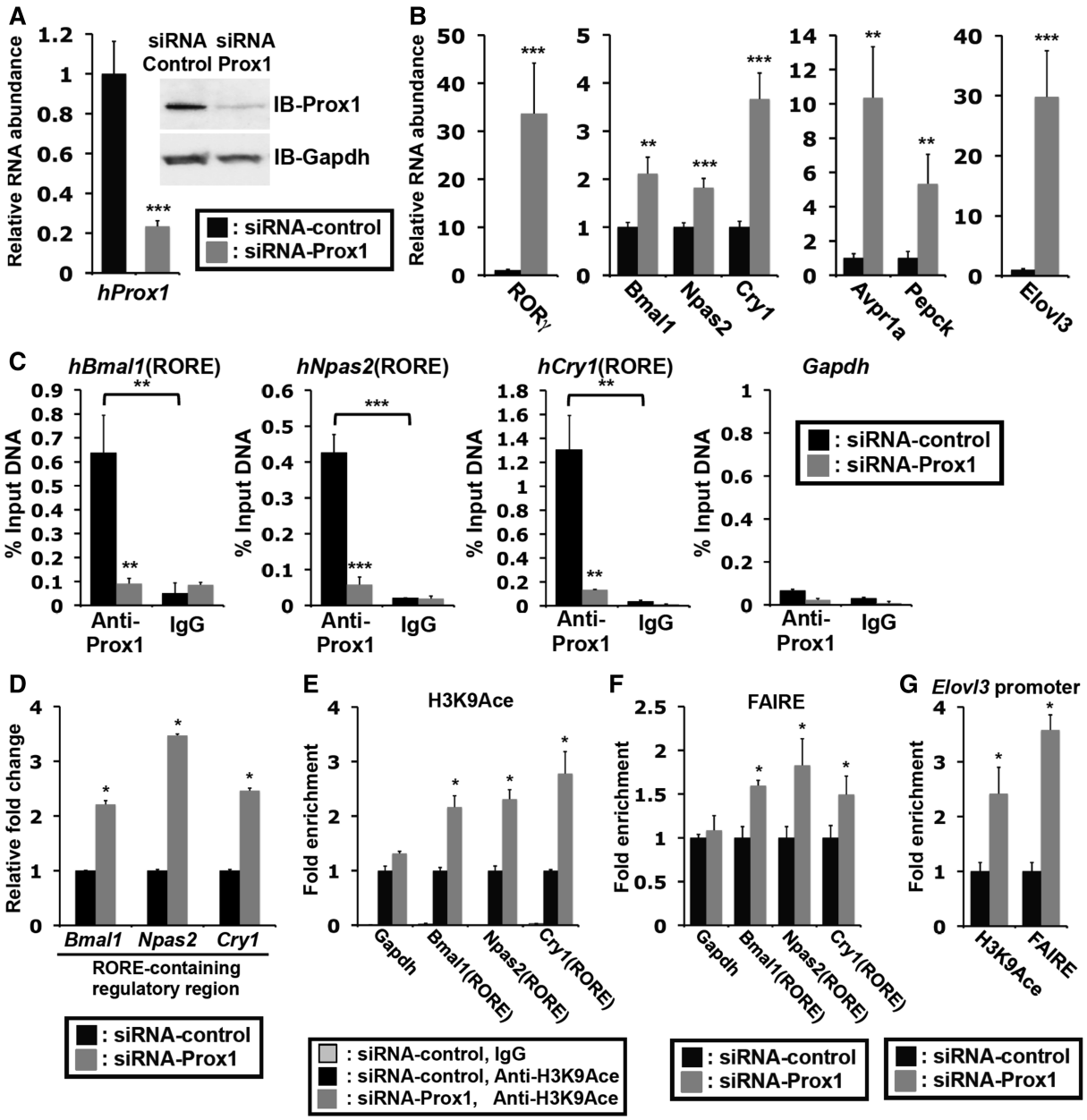

Figure 6. Prox1 represses transcription of ROR target genes. (**A**) Confirmation of the downregulation of *Prox1* mRNA and protein levels in Huh-7 cells transfected with either control siRNA or Prox1 siRNA for 3 days. *Gapdh* mRNA and protein was used as an internal control. (**B**) Effect of the downregulation of Prox1 expression on the expression of *RORγ*, *Bmal1*, *Npas2*, *Cry1*, *Avpr1a*, *Pepck* and *Elovl3*. Gene expression levels in Huh-7 cells treated with either siRNA-control or siRNA-Prox1 ($n = 3$) were analyzed by QRT–PCR. Data represent mean ± SD. (**C**) ChIP–QPCR was performed using anti-Prox1 antibody and chromatin prepared from Huh-7 treated with either siRNA-control or siRNA-Prox1 ($n = 3$). The recruitment of Prox1 to the conserved ROREs of human *Bmal1*, *Npas2* and *Cry1* was analyzed. Using non-specific IgG antibody and amplification of *Gapdh* served as a negative control. Data represent mean ± SEM, $^{**}P < 0.01$, $^{***}P < 0.001$ by ANOVA. (**D**) Effect of the downregulation of Prox1 expression on the activation of the RORE-containing regulatory regions, *Npas2*(-1534/+81), *Bmal1*(−650/+105) and *Cry1*(+22976/+23214). Huh-7 cells treated with either siRNA-control or siRNA-Prox1 were transfected with a pGL4 reporter vector under control of the indicated RORE-containing region. Relative reporter activity was analyzed 24 h later. (**E**) Increased association of H3K9Ace on the ROREs of *Bmal1*, *Npas2* and *Cry1* genes in Huh-7 cells in which Prox1 is downregulated. ChIP–QPCR analysis was performed with chromatin from Huh-7 cells treated with either siRNA-control or siRNA-Prox1 and an anti-H3K9Ace antibody. An IgG antibody and the amplification of *Gapdh* gene were used as negative controls. ChIP–QPCR data are represented as fold relative enrichment as percentage of input DNA. (**F**) Chromatin accessibility on the ROREs of *Bmal1*, *Npas2* and *Cry1* genes was assessed by FAIRE–QPCR analysis using chromatin samples prepared from Huh-7 cells treated with either siRNA-control or siRNA-Prox1. FAIRE signal is represented as fold relative enrichment as percentage of input DNA. (**G**) H3K9 acetylation and chromatin accessibility was analyzed on the proximal promoter of *Elovl3* gene as described earlier in the text. Data represent mean ± SEM; $^{*}P < 0.05$ by ANOVA.

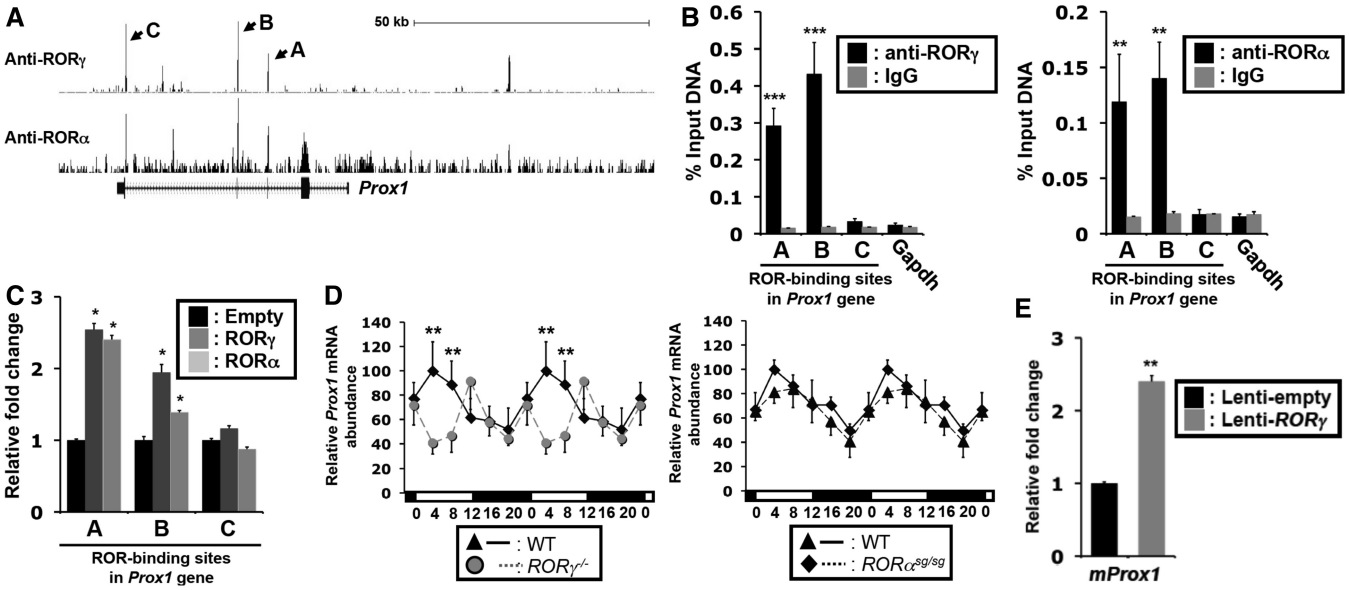

Figure 7. RORγ regulates the rhythmic expression of *Prox1*. (**A**) Genome-wide mapping of ROR-binding sites by ChIP-Seq analysis showed a strong association of both RORγ and RORα with several sites within the *Prox1* gene in mouse liver. Arrows indicate the peaks corresponding to ROR recruitment. Gene tracks were taken from the UCSC Genome Browser using the mouse mm9 reference genome. A, B and C indicate peaks common to RORα and RORγ ChIP-Seq analysis. (**B**) ChIP–QPCR was performed using either anti-RORγ or -RORα antibody and chromatin prepared from the livers ($n = 4$) collected from WT mice at ZT22. The putative ROR-binding sites A, B and C were amplified by ChIP–QPCR analysis. Amplification of *Gapdh* and a non-specific IgG antibody served as negative controls. Data represent mean ± SEM. (**C**) ROR enhanced the transactivation of the Luc reporter driven by the A and B sites. Huh-7 cells were co-transfected with pCMV-β-Gal, pCMV10-3× Flag-RORγ or -RORα and pGL4.27 reporter plasmid under the control of either the ROR-binding site A, B or C. Data represent mean ± SEM. (**D**) RORγ regulates the rhythmic expression of *Prox1*. Circadian expression of *Prox1* was analyzed by QRT–PCR in liver tissue isolated from WT, $RORγ^{-/-}$ or $RORα^{sg/sg}$ mice ($n = 4$) every 4 h over a period of 24 h. The 24 h expression pattern was double-plotted. (**E**) Exogenous expression of RORγ in mouse primary hepatocyte ($n = 3$) increased *Prox1* transcription. Data represent mean ± SD, $*P < 0.05$, $**P < 0.01$, $***P < 0.001$ by ANOVA.

knockdown might be due to both reduced repression by Prox1 and increased RORγ expression.

To determine whether reduced Prox1 expression has any effect on histone acetylation and chromatin structure, we performed a ChIP assay with an anti-H3K9Ace antibody and FAIRE analysis, which have been used as a tool to identify actively transcribed genes (58). As shown in Figure 6E–G, knockdown of Prox1 caused a 2- to 3-fold increase in H3K9Ace and FAIRE signal at the RORE-containing regions of *Bmal1*, *Npas2*, *Cry1* and the proximal promoter of *Elovl3*. These observations indicate that downregulation of Prox1 results in increased histone H3K9 acetylation and FAIRE signal, suggesting a more open chromatin structure at these regulatory sites. These results are consistent with the concept that Prox1 functions as a transcriptional repressor for RORs and modulates the expression of ROR-target genes.

Prox1 is a ROR target gene in liver

In addition to the regulation of RORγ protein stability by Prox1, we obtained evidence for transcriptional regulation of *Prox1* by RORγ. ChIP-Seq analyses with anti-RORγ or anti-RORα antibody and chromatin isolated from liver tissues at ZT22 showed that both RORγ and RORα are associated with several sites (A, B and C) in the *Prox1* gene, indicating that *Prox1* is a potential ROR target gene (Figure 7A). This was supported by ChIP-QPCR analysis showing that both RORs are recruited to the *Prox1* gene at the A and B sites, but not site C (Figure 7B). Moreover, RORs enhanced the activation of the luciferase reporter under the control of the A and B sites, but not the activation by site C (Figure 7C). In agreement with a recent report (59), *Prox1* exhibited a rhythmic pattern of expression in liver (Figure 7D). Comparison of the circadian expression of *Prox1* mRNA expression in liver from WT, $RORα^{sg/sg}$ and $RORγ^{-/-}$ mice showed that the loss of RORγ reduced the rhythmic expression of *Prox1*. Notably, the peak expression of *Prox1* mRNA during the daytime (ZT4-8) was greatly reduced in $RORγ^{-/-}$ liver, whereas the lowest level of *Prox1* expression during night time (ZT16-20) was not significantly different between WT and $RORγ^{-/-}$ liver. Despite its association with the *Prox1* gene, loss of RORα had no significant effect on the rhythmic expression of *Prox1*. Moreover, the level of *Prox1* expression in liver from $RORα^{sg/sg}RORγ^{-/-}$ double knockout mice was reduced to a similar degree as in $RORγ^{-/-}$ liver (data not shown). Inversely, overexpression of RORγ in primary hepatocyte increased *Prox1* expression (Figure 7E). Together, these results suggest that RORγ directly modulates the rhythmic expression of *Prox1 in vivo*.

DISCUSSION

In this study, we demonstrate that Prox1 interacts with both RORγ and RORα and negatively modulates the

transcriptional activity of these nuclear receptors, suggesting that it functions as a novel co-repressor of RORs. The interaction between Prox1 and RORs is supported by co-immunoprecipitation, MBP pull-down, immunocytochemistry and ChIP analysis. The co-localization of Prox1 and RORs to nuclear foci and data showing that RORγ promotes nuclear localization of Prox1 are consistent with the conclusion that these two proteins interact. Our results further demonstrated that the AF2 domain in the LBD of RORs is required for this interaction. RORγ antagonists, such as T0901317 and ursolic acid (51,52), induce a change in the conformation of the LBD of RORγ that inhibits the interaction with co-activators and enhances the recruitment of co-repressors and as a consequence repression of RORγ transcriptional activity. Likewise, the observed increase in the interaction between RORγ and Prox1 by RORγ antagonists may be due to changes in the conformation of the LBD of RORγ that result in increased stability of the RORγ–Prox1 repressor complex.

The C-terminus of Prox1 contains an atypical homeodomain and a prospero-like domain, which are critical for DNA binding and nuclear localization (30–32,34). In *Prospero*, the *Drosophila* homolog of Prox1, the prospero domain has been reported to be critical for its nuclear localization by masking a nuclear export signal within the homeodomain. MBP pull-down analysis with different deletion mutants indicated that both the N-terminus and the prospero-like domain of Prox1 can interact with RORγ (Figure 2A–C). It is well established that interaction of a number of co-repressors and co-activators with the LBD of nuclear receptors is mediated through LXXLL-like motifs (28,60). Although Prox1 contains two such motifs at its N-terminus between amino acids 70 and 96, mutation and deletion analysis indicated that they were not required for its interaction with RORγ. Instead, the first 28 amino acids at the N-terminus of Prox1 were sufficient to mediate the interaction with RORγ.

Analysis of the subcellular localization of Prox1 showed that loss of either its N- or C-terminus reduced the nuclear localization of Prox1. However, the loss of the C-terminus had a larger effect, suggesting that the C-terminus is more critical in controlling Prox1 nuclear localization than its N-terminus. Co-expression with RORγ greatly enhanced the nuclear localization of Prox1 mutants lacking either the prospero-like domain or the N-terminus, but not of the mutant lacking both the N- and C-terminus (Figure 3C–F and Supplementary Figure S3). Moreover, deletion of the 28 N-terminal amino acids in PΔC636 abrogated the ability of RORγ to promote Prox1 nuclear localization. In contrast, mutations in the LXXLL motifs of Prox1 had little effect on the RORγ-mediated increase in Prox1 nuclear localization, suggesting that the LXXLL motifs of Prox1 are not required (Supplementary Figure S3A). Analysis of additional deletions within the prospero-like domain of PΔN106 indicated that the region between ^{723}Glu and ^{729}Asn, which in *Drosophila Prospero* contains a small α-helix (34), is required for the interaction with RORγ as well the increased nuclear localization of Prox1 by RORγ (Figure 3G–I). These data indicate that there is a strong correlation between the regions mediating the interaction of Prox1 with RORγ (Figure 2) and the ones needed for RORγ to promote Prox1 nuclear localization (Figure 3). These observations are consistent with the conclusion that RORγ promotes the nuclear localization of Prox1 by interacting with either its C- or N-terminus.

Although several studies have demonstrated that Prox1 interacts with a select group of other nuclear receptors, there are clear differences in the manner by which they interact. Like RORs, the interaction of Prox1 with the nuclear receptors, HNF4α, LRH-1 and PXR, was mediated through their LBD domain, whereas the interaction with ERRα occurred through its DBD (36,37,56,61). The interaction of Prox1 with HNF4α and LRH-1 requires its LXXLL motifs; however, like ERRα and PXR, the interaction of Prox1 with RORs was independent of the LXXLL motifs. These findings indicate that the mechanisms by which Prox1 interacts with nuclear receptors are distinct between receptors; however, in all cases, Prox1 functions as a repressor of transcriptional activation.

Prox1 has been reported to function either as a transcriptional activator or as a repressor (35–37,55,61–64). Prox1 can mediate its effect on gene transcription either by binding directly to its DNA elements or indirectly through protein–protein interactions. Our study demonstrates that the interaction of Prox1 with RORs results in a repression of RORE-dependent and *Npas2*(RORE)-driven transcriptional activation by RORs, indicating that Prox1 functions as a novel co-repressor of RORs (Figure 4A and B). This conclusion is supported by mammalian monohybrid analysis showing that Prox1 inhibited UAS-dependent transcriptional activation by Gal4(DBD)-RORγ(LBD). Prox1 also repressed the UAS-driven transactivation that is dependent on the interaction of Gal4(DBD)-LXXLL(EBIP96) and VP16-RORγ(LBD), suggesting that Prox1 decreased this activation by inhibiting the interaction between RORγ and LXXLL peptides and co-activators (Figure 4C and D). In contrast, Prox1 did not repress the transcriptional activation by the nuclear receptor TAK1, suggesting that Prox1 acts selectively and is not a general inhibitor of the basic transcriptional machinery (Supplementary Figure S4B). Analysis of different deletions and mutations in Prox1 demonstrated that although the 106 amino acids N-terminus of Prox1 can interact with RORγ, deletion of the N-terminus had no significant effect on the inhibition of RORγ activity, suggesting that the N-terminus, which includes the LXXLL motifs, is not essential for this function (Figure 4F). However, deletion of the homeo/prospero-like domain or only the prospero-like domain abolished the ability of Prox1 to repress RORγ-induced transactivation. Particularly the ^{723}Glu and ^{729}Asn region of the prospero-like domain is required for this repression. Our data further showed that N626A/R628A mutations in the homeodomain, which destroy the ability of the homeodomain to bind DNA (55), abolished Prox1 repressor activity. Because no apparent Prox1-binding sequence could be identified in the synthetic RORE- and UAS-containing promoters or in the RORE-containing

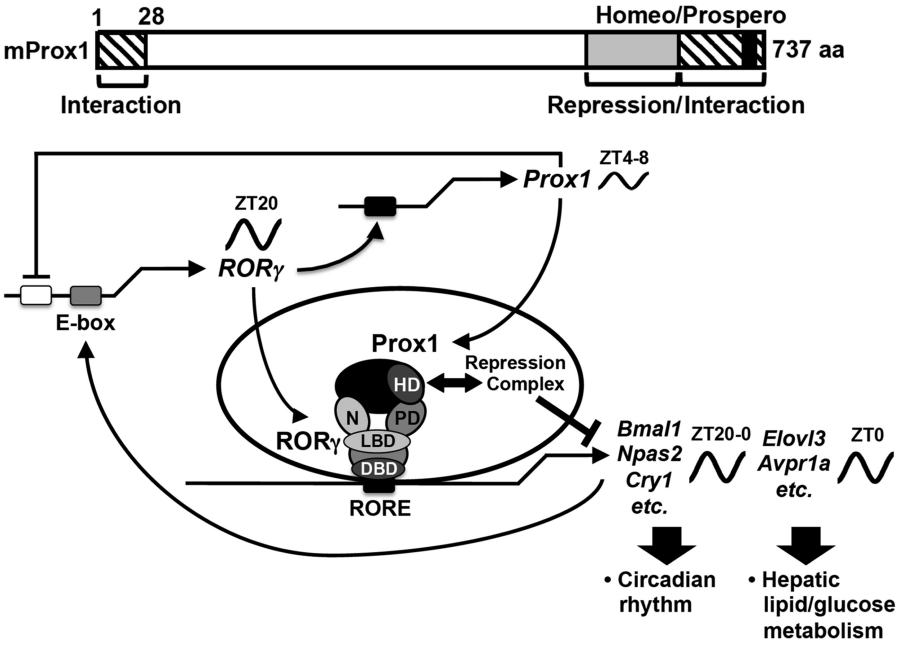

Figure 8. Schematic model of the interrelationship between RORs, Prox1 and the circadian and metabolic networks. Prox1 interacts directly with RORα and RORγ. The AF2 domain of RORs and the N-terminal 28 amino acids and the prospero-like domain of Prox1, particularly the ^{723}EIFKSPN^{729} region (black box), are mediating this interaction. Prox1 is able to repress the activation and expression of RORγ target genes. The homeo/prospero-like domain of Prox1 is essential for this repression. Prox1 is recruited by RORs to ROREs in the RORE-containing regulatory regions of ROR target genes, including several circadian clock and metabolic genes, suggesting that it functions as a negative regulator of RORγ-mediated transcription. Prox1 also functions as a repressor of *RORγ* transcription as indicated by data showing that Prox1 knockdown significantly enhanced *RORγ* mRNA expression and by the recruitment of Prox1 to the *RORγ* promoter (59). Inversely, RORγ functions as a positive regulator of *Prox1* transcription. This is supported by the repression of the *Prox1* expression in *RORγ*$^{-/-}$ mice, the recruitment of RORs to the *Prox1* gene and the increased expression of Prox1 by exogenously expressed RORγ. Our observations suggest that Prox1 and RORγ are part of a feedback loop in which RORγ positively regulates *Prox1* and Prox1 negatively regulates RORγ. Modulation of the rhythmic expression of *Prox1* by RORγ and their regulation of several clock and metabolic genes supports a role for both RORγ and Prox1 in the control of circadian rhythm and metabolism. Prox1 is increasing when RORγ-target gene expression (e.g. *Bmal1*, *Npas2*, *Avpr1a* and *Elovl3*) peak at ZT0. Prox1 reaches optimum expression at ZT4 when these genes are downregulated. We propose that by inhibiting RORγ transcriptional activity and expression, increased expression of Prox1 might contribute to the downregulation of RORγ target genes, including several clock and metabolic genes. N, HD and PD refer to the N-terminus, homeodomain and prospero-like domain of Prox1, respectively.

regulatory regions of several clock genes, it seems unlikely that direct interaction of Prox1 with DNA is involved in the repression of RORγ-mediated transactivation reported in this study. However, we cannot rule out that in certain instances, binding of Prox1 to DNA may be involved in the repression of RORγ activity. We propose that the homeodomain might mediate the interaction with additional proteins within the co-repressor complex recruited by RORγ. Together our findings indicate that the homeo/prospero-like domain of Prox1 is critical for its repression of RORγ-mediated transactivation (Figure 8).

RORγ and Prox1 are co-expressed in several tissues, including liver (15,57). Recent studies have shown an interrelationship between the ROR regulatory network and the controls of circadian rhythm and metabolic homeostasis (8,20,65). RORs are involved in the regulation of the rhythmic expression of several clock genes, including *Npas2*, *Bmal1* and *Cry1,* and various metabolic genes, such as *Avpr1a* and *Elovl3* (7,9–13,15). Recently, promoter, ChIP–QPCR and ChIP-Seq analysis demonstrated that RORs, and RORγ in particular, are associated with ROREs in the regulatory regions of these genes, indicating that their transcription is directly regulated by RORs (9,10,12,13). The repression of the ROR-induced activation of *Bmal1*(RORE), *Cry1*(RORE) (Supplementary Figure S4A) and the *Npas2*(RORE) promoter (Figure 4) by Prox1 observed in this study is consistent with a role for this co-repressor in the negative regulation of clock gene expression and downstream metabolic outputs (Figure 8). This conclusion was supported by data showing that knockdown of Prox1 by corresponding siRNAs in human hepatoma Huh-7 cells resulted in enhanced expression of several ROR-targets, including the clock genes, *Bmal1*, *Npas2* and *Cry1*, as well as the metabolic genes, *Avpr1a* and *Elovl3* (Figure 6B). These observations suggest a link between RORs, Prox1 and the regulation of clock gene expression and downstream metabolic pathways (Figure 8). This conclusion is consistent with a recent study providing evidence for a link between ERRα, Prox1 and the control of metabolic clock outputs (56,59).

ChIP–QPCR analysis indicated that in liver Prox1 is associated with the RORE-containing regulatory regions in *Bmal1*, *Npas2* and *Cry1*, consistent with our observations that Prox1 interacts with RORs and functions as a ROR co-repressor (Figure 5A). Prox1 was also recruited to the RORE-containing regulatory regions of clock genes

in human hepatoma cells (Figure 6C). Re-ChIP analysis supported the conclusion that at these sites RORs, and Prox1 is part of the same complex (Figure 5C). Prox1 was less efficiently recruited to these RORE sites in RORγ-deficient mice, suggesting that the recruitment of Prox1 is at least partially dependent on RORγ. The residual recruitment of Prox1 might be mediated through RORα, which also binds these ROREs (10). We further showed that the association of Prox1 with these regulatory regions was ZT-dependent and was higher at ZT20 than at ZT8 correlating with the level of expression and recruitment of RORγ to these sites (9,10) (Figure 5B). FAIRE analysis, which assesses chromatin accessibility, showed that the FAIRE–QPCR signal on the RORE-containing regulatory regions of the ROR target genes *Bmal1*, *Npas2*, *Cry1* and *Elovl3*, was significantly increased in Huh-7 cells in which Prox1 expression was knockeddown by respective siRNA but was not changed at the *Gapdh* promoter (Figure 6E and F). These data are consistent with the concept that these regions exhibit a more open chromatin structure and are more accessible for transcription. This was supported by ChIP analysis showing that the level of H3K9Ace associated with these RORE-containing regulatory sites was considerably higher in cells in which Prox1 was downregulated (Figure 6D and F). These observations suggest that recruitment of Prox1 to regulatory regions correlates with a more closed chromatin structure consistent with the repressor function of Prox1.

Besides the observations that Prox1 interacts with RORγ and modulates RORγ activity, it also regulates the expression of RORγ, as indicated by data showing that knockdown of *Prox1* significantly increased the level of *RORγ* mRNA in human hepatoma cells (Figure 6B). Interestingly, a recent study (59) analyzing the association of Prox1 with chromatin revealed that Prox1 protein was recruited to the *RORγ* gene. These findings are consistent with the concept that Prox1 regulates *RORγ* transcription. Inversely, our results demonstrated that the expression of *Prox1* itself is regulated by RORγ. The rhythmic expression of *Prox1*, which reaches a peak at ZT4, was largely abolished in liver of *RORγ*-deficient mice, whereas loss of RORα had little effect (Figure 7C). Thus, as we reported previously for several clock and metabolic genes (10), RORγ rather than RORα regulates the oscillatory expression of *Prox1*. ChIP-Seq and ChIP-QPCR analysis revealed that RORγ was associated with at least two sites within the *Prox1* gene, suggesting that it might be directly regulated by RORγ (Figure 7A and B). The latter was supported by data showing that RORγ was able to enhance the activation of a reporter controlled by these regions, and that exogenous expression of RORγ in primary mouse hepatocytes increased the level of endogenous *Prox1* mRNA (Figure 7C). The mutual regulation of RORγ and Prox1 suggests that Prox1 and RORγ are part of a feedback loop in which RORγ enhances the expression of *Prox1*, which in turn represses the activity and transcription of *RORγ* (Figure 8). Increased RORγ expression at ZT20 has been reported to positively regulate *Bmal1*, *Npas2* and *Cry1* during ZT20-0 (10). The expression of Prox1 is increasing when the expression of RORγ target genes (e.g. *Bmal1*, *Npas2* and metabolic genes, *Avpr1a* and *Elovl3*) peak. Prox1 reaches optimum expression at ZT4 during a time when the expression of these RORγ target genes is downregulated. We propose that by inhibiting RORγ transcriptional activity and expression, increased expression of Prox1 might contribute to the downregulation of these RORγ target genes. The RORγ–Prox1 feedback mechanism is reminiscent of other feedback loops regulating the circadian molecular clock, including the loops consisting of Bmal1/Clock, Per, Cry1 and Rev-Erbs (66,67) and is consistent with a role for RORs and Prox1 in the regulation of circadian rhythm (8–14,59,65).

In summary, our results demonstrate that Prox1 interacts with ROR nuclear receptors and represses the transcriptional activity of RORγ and expression of RORγ, thereby contributing to the downregulation of several ROR target genes. The AF2 in the LBD of RORs and the homeo/propero-like domain of Prox1 are required for the interaction, as well as repression. Our study identifies Prox1 as a novel modulator of ROR transcriptional regulation and as such is an integral part of the circadian clock and metabolic regulatory networks.

SUPPLEMENTARY DATA

Supplementary Data are available at NAR Online: Supplementary Tables 1 and 2 and Supplementary Figures 1–4.

ACKNOWLEDGEMENTS

The authors thank Dr Kristin Lichti-Kaiser, Dr Gary ZeRuth and Dr Tatsuya Sueyoshi for their comments on the manuscript and Laura Miller (NIEHS) for her assistance with the mice.

FUNDING

Intramural Research Program of the National Institute of Environmental Health Sciences, the National Institutes of Health (NIH) [Z01-ES-101586] and the Japanese Society for the Promotion of Science (JSPS). Funding for open access charge: NIH.

Conflict of interest statement. None declared.

REFERENCES

1. Kallen,J.A., Schlaeppi,J.M., Bitsch,F., Geisse,S., Geiser,M., Delhon,I. and Fournier,B. (2002) X-ray structure of the hRORalpha LBD at 1.63 A: structural and functional data that cholesterol or a cholesterol derivative is the natural ligand of RORalpha. *Structure*, **10**, 1697–1707.
2. Jetten,A.M. (2011) Immunology: a helping hand against autoimmunity. *Nature*, **472**, 421–422.
3. Solt,L.A., Wang,Y., Banerjee,S., Hughes,T., Kojetin,D.J., Lundasen,T., Shin,Y., Liu,J., Cameron,M.D., Noel,R. *et al.* (2012) Regulation of circadian behaviour and metabolism by synthetic REV-ERB agonists. *Nature*, **485**, 62–68.
4. Jetten,A.M. (2009) Retinoid-related orphan receptors (RORs): critical roles in development, immunity, circadian rhythm, and cellular metabolism. *Nucl. Recept. Signal.*, **7**, e003.

5. Huh,J.R. and Littman,D.R. (2012) Small molecule inhibitors of RORgammat: targeting Th17 cells and other applications. *Eur. J. Immunol.*, **42**, 2232–2237.
6. Sato,T.K., Panda,S., Miraglia,L.J., Reyes,T.M., Rudic,R.D., McNamara,P., Naik,K.A., FitzGerald,G.A., Kay,S.A. and Hogenesch,J.B. (2004) A functional genomics strategy reveals Rora as a component of the mammalian circadian clock. *Neuron*, **43**, 527–537.
7. Ueda,H.R., Hayashi,S., Chen,W., Sano,M., Machida,M., Shigeyoshi,Y., Iino,M. and Hashimoto,S. (2005) System-level identification of transcriptional circuits underlying mammalian circadian clocks. *Nat. Genet.*, **37**, 187–192.
8. Duez,H. and Staels,B. (2010) Nuclear receptors linking circadian rhythms and cardiometabolic control. *Arterioscler. Thromb. Vac. Biol.*, **30**, 1529–1534.
9. Takeda,Y., Kang,H.S., Angers,M. and Jetten,A.M. (2011) Retinoic acid-related orphan receptor gamma directly regulates neuronal PAS domain protein 2 transcription *in vivo*. *Nucleic Acids Res.*, **39**, 4769–4782.
10. Takeda,Y., Jothi,R., Birault,V. and Jetten,A.M. (2012) RORgamma directly regulates the circadian expression of clock genes and downstream targets *in vivo*. *Nucleic Acids Res.*, **40**, 8519–8535.
11. Akashi,M. and Takumi,T. (2005) The orphan nuclear receptor RORalpha regulates circadian transcription of the mammalian core-clock Bmal1. *Nat. Struct. Mol. Biol.*, **12**, 441–448.
12. Crumbley,C., Wang,Y., Kojetin,D.J. and Burris,T.P. (2010) Characterization of the core mammalian clock component, NPAS2, as a REV-ERBalpha/RORalpha target gene. *J. Biol. Chem.*, **285**, 35386–35392.
13. Guillaumond,F., Dardente,H., Giguere,V. and Cermakian,N. (2005) Differential control of Bmal1 circadian transcription by REV-ERB and ROR nuclear receptors. *J. Biol. Rhythms*, **20**, 391–403.
14. Muhlbauer,E., Bazwinsky-Wutschke,I., Wolgast,S., Labucay,K. and Peschke,E. (2013) Differential and day-time dependent expression of nuclear receptors RORalpha, RORbeta, RORgamma and RXRalpha in the rodent pancreas and islet. *Mol. Cell. Endocrinol.*, **365**, 129–138.
15. Kang,H.S., Angers,M., Beak,J.Y., Wu,X., Gimble,J.M., Wada,T., Xie,W., Collins,J.B., Grissom,S.F. and Jetten,A.M. (2007) Gene expression profiling reveals a regulatory role for ROR alpha and ROR gamma in phase I and phase II metabolism. *Physiol. Genomics*, **31**, 281–294.
16. Wada,T., Kang,H.S., Angers,M., Gong,H., Bhatia,S., Khadem,S., Ren,S., Ellis,E., Strom,S.C., Jetten,A.M. *et al.* (2008) Identification of oxysterol 7alpha-hydroxylase (Cyp7b1) as a novel retinoid-related orphan receptor alpha (RORalpha) (NR1F1) target gene and a functional cross-talk between RORalpha and liver X receptor (NR1H3). *Mol. Pharmacol.*, **73**, 891–899.
17. Kang,H.S., Okamoto,K., Takeda,Y., Beak,J.Y., Gerrish,K., Bortner,C.D., DeGraff,L.M., Wada,T., Xie,W. and Jetten,A.M. (2011) Transcriptional profiling reveals a role for RORalpha in regulating gene expression in obesity-associated inflammation and hepatic steatosis. *Physiol. Genomics*, **43**, 818–828.
18. Lau,P., Fitzsimmons,R.L., Raichur,S., Wang,S.C., Lechtken,A. and Muscat,G.E. (2008) The orphan nuclear receptor, RORalpha, regulates gene expression that controls lipid metabolism: staggerer (SG/SG) mice are resistant to diet-induced obesity. *J. Biol. Chem.*, **283**, 18411–18421.
19. Fitzsimmons,R.L., Lau,P. and Muscat,G.E. (2012) Retinoid-related orphan receptor alpha and the regulation of lipid homeostasis. *J. Steroid Biochem. Mol. Biol.*, **130**, 159–168.
20. Jetten,A.M., Kang,H.S. and Takeda,Y. (2013) Retinoic acid-related orphan receptors alpha and gamma: key regulators of lipid/glucose metabolism, inflammation, and insulin sensitivity. *Front. Endocrinol.*, **4**, 1–8.
21. Meissburger,B., Ukropec,J., Roeder,E., Beaton,N., Geiger,M., Teupser,D., Civan,B., Langhans,W., Nawroth,P.P., Gasperikova,D. *et al.* (2011) Adipogenesis and insulin sensitivity in obesity are regulated by retinoid-related orphan receptor gamma. *EMBO Mol. Med.*, **3**, 637–651.
22. Tinahones,F.J., Moreno-Santos,I., Vendrell,J., Chacon,M.R., Garrido-Sanchez,L., Garcia-Fuentes,E. and Macias-Gonzalez,M. (2012) The retinoic acid receptor-related orphan nuclear receptor gamma1 (RORgamma1): a novel player determinant of insulin sensitivity in morbid obesity. *Obesity*, **20**, 488–497.
23. Le-Niculescu,H., Patel,S.D., Bhat,M., Kuczenski,R., Faraone,S.V., Tsuang,M.T., McMahon,F.J., Schork,N.J., Nurnberger,J.I. Jr and Niculescu,A.B. (2009) Convergent functional genomics of genome-wide association data for bipolar disorder: comprehensive identification of candidate genes, pathways and mechanisms. *Am. J. Med. Genet. B Neuropsychiatr. Genet.*, **150B**, 155–181.
24. Medrano,L.M., Garcia-Magarinos,M., Dema,B., Espino,L., Maluenda,C., Polanco,I., Figueredo,M.A., Fernandez-Arquero,M. and Nunez,C. (2012) Th17-related genes and celiac disease susceptibility. *PLoS One*, **7**, e31244.
25. Ramasamy,A., Kuokkanen,M., Vedantam,S., Gajdos,Z.K., Couto Alves,A., Lyon,H.N., Ferreira,M.A., Strachan,D.P., Zhao,J.H., Abramson,M.J. *et al.* (2012) Genome-wide association studies of asthma in population-based cohorts confirm known and suggested loci and identify an additional association near HLA. *PLoS One*, **7**, e44008.
26. Gamboa-Melendez,M.A., Huerta-Chagoya,A., Moreno-Macias,H., Vazquez-Cardenas,P., Ordonez-Sanchez,M.L., Rodriguez-Guillen,R., Riba,L., Rodriguez-Torres,M., Guerra-Garcia,M.T., Guillen-Pineda,L.E. *et al.* (2012) Contribution of common genetic variation to the risk of type 2 diabetes in the Mexican Mestizo population. *Diabetes*, **61**, 3314–3321.
27. Albers,M., Kranz,H., Kober,I., Kaiser,C., Klink,M., Suckow,J., Kern,R. and Koegl,M. (2005) Automated yeast two-hybrid screening for nuclear receptor-interacting proteins. *Mol. Cell. Proteomics*, **4**, 205–213.
28. Kurebayashi,S., Nakajima,T., Kim,S.C., Chang,C.Y., McDonnell,D.P., Renaud,J.P. and Jetten,A.M. (2004) Selective LXXLL peptides antagonize transcriptional activation by the retinoid-related orphan receptor RORgamma. *Biochem. Biophys. Res. Commun.*, **315**, 919–927.
29. Liu,C., Li,S., Liu,T., Borjigin,J. and Lin,J.D. (2007) Transcriptional coactivator PGC-1alpha integrates the mammalian clock and energy metabolism. *Nature*, **447**, 477–481.
30. Elsir,T., Smits,A., Lindstrom,M.S. and Nister,M. (2012) Transcription factor PROX1: its role in development and cancer. *Cancer Metastasis Rev.*, **31**, 795–805.
31. Nishijima,I. and Ohtoshi,A. (2006) Characterization of a novel prospero-related homeobox gene, Prox2. *Mol. Genet. Genomics*, **275**, 471–478.
32. Bi,X., Kajava,A.V., Jones,T., Demidenko,Z.N. and Mortin,M.A. (2003) The carboxy terminus of Prospero regulates its subcellular localization. *Mol. Cell. Biol.*, **23**, 1014–1024.
33. Demidenko,Z., Badenhorst,P., Jones,T., Bi,X. and Mortin,M.A. (2001) Regulated nuclear export of the homeodomain transcription factor Prospero. *Development*, **128**, 1359–1367.
34. Ryter,J.M., Doe,C.Q. and Matthews,B.W. (2002) Structure of the DNA binding region of prospero reveals a novel homeo-prospero domain. *Structure*, **10**, 1541–1549.
35. Yousef,M.S. and Matthews,B.W. (2005) Structural basis of Prospero-DNA interaction: implications for transcription regulation in developing cells. *Structure*, **13**, 601–607.
36. Song,K.H., Li,T. and Chiang,J.Y. (2006) A Prospero-related homeodomain protein is a novel co-regulator of hepatocyte nuclear factor 4alpha that regulates the cholesterol 7alpha-hydroxylase gene. *J. Biol. Chem.*, **281**, 10081–10088.
37. Steffensen,K.R., Holter,E., Bavner,A., Nilsson,M., Pelto-Huikko,M., Tomarev,S. and Treuter,E. (2004) Functional conservation of interactions between a homeodomain cofactor and a mammalian FTZ-F1 homologue. *EMBO Rep.*, **5**, 613–619.
38. Yoshimatsu,Y., Yamazaki,T., Mihira,H., Itoh,T., Suehiro,J., Yuki,K., Harada,K., Morikawa,M., Iwata,C., Minami,T. *et al.* (2011) Ets family members induce lymphangiogenesis through physical and functional interaction with Prox1. *J. Cell Sci.*, **124**, 2753–2762.
39. Francois,M., Harvey,N.L. and Hogan,B.M. (2011) The transcriptional control of lymphatic vascular development. *Physiology*, **26**, 146–155.
40. Karalay,O., Doberauer,K., Vadodaria,K.C., Knobloch,M., Berti,L., Miquelajauregui,A., Schwark,M., Jagasia,R., Taketo,M.M., Tarabykin,V. *et al.* (2011) Prospero-related

homeobox 1 gene (Prox1) is regulated by canonical Wnt signaling and has a stage-specific role in adult hippocampal neurogenesis. *Proc. Natl Acad. Sci. USA*, **108**, 5807–5812.
41. Sosa-Pineda,B., Wigle,J.T. and Oliver,G. (2000) Hepatocyte migration during liver development requires Prox1. *Nat. Genet.*, **25**, 254–255.
42. Westmoreland,J.J., Kilic,G., Sartain,C., Sirma,S., Blain,J., Rehg,J., Harvey,N. and Sosa-Pineda,B. (2011) Pancreas-specific deletion of Prox1 affects development and disrupts homeostasis of the exocrine pancreas. *Gastroenterology*, **142**, 999–1009.
43. Wang,J., Kilic,G., Aydin,M., Burke,Z., Oliver,G. and Sosa-Pineda,B. (2005) Prox1 activity controls pancreas morphogenesis and participates in the production of "secondary transition" pancreatic endocrine cells. *Dev. Biol.*, **286**, 182–194.
44. Petrova,T.V., Nykanen,A., Norrmen,C., Ivanov,K.I., Andersson,L.C., Haglund,C., Puolakkainen,P., Wempe,F., von Melchner,H., Gradwohl,G. *et al.* (2008) Transcription factor PROX1 induces colon cancer progression by promoting the transition from benign to highly dysplastic phenotype. *Cancer Cell*, **13**, 407–419.
45. Dupuis,J., Langenberg,C., Prokopenko,I., Saxena,R., Soranzo,N., Jackson,A.U., Wheeler,E., Glazer,N.L., Bouatia-Naji,N., Gloyn,A.L. *et al.* (2010) New genetic loci implicated in fasting glucose homeostasis and their impact on type 2 diabetes risk. *Nat. Genet.*, **42**, 105–116.
46. Ohshige,T., Iwata,M., Omori,S., Tanaka,Y., Hirose,H., Kaku,K., Maegawa,H., Watada,H., Kashiwagi,A., Kawamori,R. *et al.* (2011) Association of new loci identified in European genome-wide association studies with susceptibility to type 2 diabetes in the Japanese. *PLoS One*, **6**, e26911.
47. Lecompte,S., Pasquetti,G., Hermant,X., Grenier-Boley,B., Gonzalez-Gross,M., De Henauw,S., Molnar,D., Stehle,P., Beghin,L., Moreno,L.A. *et al.* (2013) Genetic and molecular insights into the role of PROX1 in glucose metabolism. *Diabetes*, **62**, 1738–1745.
48. Dussault,I., Fawcett,D., Matthyssen,A., Bader,J.A. and Giguere,V. (1998) Orphan nuclear receptor ROR alpha-deficient mice display the cerebellar defects of staggerer. *Mech. Dev.*, **70**, 147–153.
49. Kurebayashi,S., Ueda,E., Sakaue,M., Patel,D.D., Medvedev,A., Zhang,F. and Jetten,A.M. (2000) Retinoid-related orphan receptor gamma (RORgamma) is essential for lymphoid organogenesis and controls apoptosis during thymopoiesis. *Proc. Natl Acad. Sci. USA*, **97**, 10132–10137.
50. Nakajima,T., Fujino,S., Nakanishi,G., Kim,Y.S. and Jetten,A.M. (2004) TIP27: a novel repressor of the nuclear orphan receptor TAK1/TR4. *Nucleic Acids Res*, **32**, 4194–4204.
51. Kumar,N., Solt,L.A., Conkright,J.J., Wang,Y., Istrate,M.A., Busby,S.A., Garcia-Ordonez,R.D., Burris,T.P. and Griffin,P.R. (2010) The benzenesulfoamide T0901317 [N-(2,2,2-trifluoroethyl)-N-[4-[2,2,2-trifluoro-1-hydroxy-1-(trifluoromethyl)ethyl] phenyl]-benzenesulfonamide] is a novel retinoic acid receptor-related orphan receptor-alpha/gamma inverse agonist. *Mol. Pharmacol.*, **77**, 228–236.
52. Xu,T., Wang,X., Zhong,B., Nurieva,R.I., Ding,S. and Dong,C. (2011) Ursolic acid suppresses interleukin-17 (IL-17) production by selectively antagonizing the function of RORgamma t protein. *J. Biol. Chem.*, **286**, 22707–22710.
53. McInerney,E.M., Rose,D.W., Flynn,S.E., Westin,S., Mullen,T.M., Krones,A., Inostroza,J., Torchia,J., Nolte,R.T., Assa-Munt,N. *et al.* (1998) Determinants of coactivator LXXLL motif specificity in nuclear receptor transcriptional activation. *Genes Dev.*, **12**, 3357–3368.
54. Heery,D.M., Hoare,S., Hussain,S., Parker,M.G. and Sheppard,H. (2001) Core LXXLL motif sequences in CREB-binding protein, SRC1, and RIP140 define affinity and selectivity for steroid and retinoid receptors. *J. Biol. Chem.*, **276**, 6695–6702.
55. Shin,J.W., Min,M., Larrieu-Lahargue,F., Canron,X., Kunstfeld,R., Nguyen,L., Henderson,J.E., Bikfalvi,A., Detmar,M. and Hong,Y.K. (2006) Prox1 promotes lineage-specific expression of fibroblast growth factor (FGF) receptor-3 in lymphatic endothelium: a role for FGF signaling in lymphangiogenesis. *Mol. Biol. Cell*, **17**, 576–584.
56. Charest-Marcotte,A., Dufour,C.R., Wilson,B.J., Tremblay,A.M., Eichner,L.J., Arlow,D.H., Mootha,V.K. and Giguere,V. (2010) The homeobox protein Prox1 is a negative modulator of ERR{alpha}/PGC-1{alpha} bioenergetic functions. *Genes Dev.*, **24**, 537–542.
57. Zinovieva,R.D., Duncan,M.K., Johnson,T.R., Torres,R., Polymeropoulos,M.H. and Tomarev,S.I. (1996) Structure and chromosomal localization of the human homeobox gene Prox 1. *Genomics*, **35**, 517–522.
58. Giresi,P.G., Kim,J., McDaniell,R.M., Iyer,V.R. and Lieb,J.D. (2007) FAIRE (Formaldehyde-Assisted Isolation of Regulatory Elements) isolates active regulatory elements from human chromatin. *Genome Res.*, **17**, 877–885.
59. Dufour,C.R., Levasseur,M.P., Pham,N.H., Eichner,L.J., Wilson,B.J., Charest-Marcotte,A., Duguay,D., Poirier-Heon,J.F., Cermakian,N. and Giguere,V. (2011) Genomic convergence among ERRalpha, PROX1, and BMAL1 in the control of metabolic clock outputs. *PLoS Genet.*, **7**, e1002143.
60. Heery,D.M., Kalkhoven,E., Hoare,S. and Parker,M.G. (1997) A signature motif in transcriptional co-activators mediates binding to nuclear receptors. *Nature*, **387**, 733–736.
61. Azuma,K., Urano,T., Watabe,T., Ouchi,Y. and Inoue,S. (2011) PROX1 suppresses vitamin K-induced transcriptional activity of Steroid and Xenobiotic Receptor. *Genes Cell*, **16**, 1063–1070.
62. Baxter,S.A., Cheung,D.Y., Bocangel,P., Kim,H.K., Herbert,K., Douville,J.M., Jangamreddy,J.R., Zhang,S., Eisenstat,D.D. and Wigle,J.T. (2011) Regulation of the lymphatic endothelial cell cycle by the PROX1 homeodomain protein. *Biochim. Biophys. Acta*, **1813**, 201–212.
63. Pan,M.R., Chang,T.M., Chang,H.C., Su,J.L., Wang,H.W. and Hung,W.C. (2009) Sumoylation of Prox1 controls its ability to induce VEGFR3 expression and lymphatic phenotypes in endothelial cells. *J. Cell Sci.*, **122**, 3358–3364.
64. Risebro,C.A., Petchey,L.K., Smart,N., Gomes,J., Clark,J., Viera,J.M., Yanni,J., Dobrzynski,H., Davidson,S., Zuberi,Z. *et al.* (2012) Epistatic rescue of Nkx2.5 adult cardiac conduction disease phenotypes by Prospero-related homeobox protein 1 and HDAC3. *Circ. Res.*, **111**, e19–e31.
65. Solt,L.A., Kojetin,D.J. and Burris,T.P. (2011) The REV-ERBs and RORs: molecular links between circadian rhythms and lipid homeostasis. *Future Med. Chem.*, **3**, 623–638.
66. Asher,G. and Schibler,U. (2011) Crosstalk between components of circadian and metabolic cycles in mammals. *Cell Metab.*, **13**, 125–137.
67. Bass,J. and Takahashi,J.S. (2010) Circadian integration of metabolism and energetics. *Science*, **330**, 1349–1354.